Available online at www.sciencedirect.com
SCIENCE DIRECT
Continental Shelf Research 24 (2004) 859–897
CONTINENTAL SHELF RESEARCH
www.elsevier.com/locate/csr

Meteorology and oceanography of the Northern Gulf of Alaska

P.J. Stabeno[a,*], N.A. Bond[b], A.J. Hermann[b], N.B. Kachel[b], C.W. Mordy[b], J.E. Overland[a]

[a] *Pacific Marine Environmental Laboratory/NOAA, 7600 Sand Point Way NE, Seattle, WA 98115, USA*
[b] *JISAO/University of Washington and PMEL, 7600 Sand Point Way NE, Seattle, WA 98115, USA*

Abstract

The Gulf of Alaska shelf is dominated by the Alaska Coastal current (ACC), which is forced by along-shore winds and large freshwater runoff. Strong cyclonic winds dominate from fall through spring, and substantial runoff occurs from late spring through fall with annual distributed freshwater discharge greater than that of the Mississippi River. We examine the ACC from Icy Bay to Unimak Pass, a distance of over 1500 km. Over this distance, the ACC is a nearly continuous feature with a marked freshwater core. The annual mean transport, as measured from current meters, is approximately $1.0 \times 10^6\,m^3\,s^{-1}$ along the Kenai Peninsula, with transport decreasing as the ACC travels westward. Even though the coastal GOA is a predominately downwelling system, it supports a productive ecosystem. Macro nutrients from the basin are provided to the coastal system through a number of processes including topographic steering, eddies, upwelling in response to horizontal shear in the barrier jets, and during winter the on-shelf flux in the surface Ekman layer. Micronutrients (e.g., iron) are supplied from mechanisms such as resuspension of shelf sediments and river discharge. While strong seasonal cycles and interannual variability are dominant scales in atmospheric forcing and the oceanic response, there is also forcing on ENSO and decadal time scales.

Keywords: Gulf of Alaska; Alaska Coastal Current; Alaskan Stream; Cross-shelf mechanisms; Coastal winds

1. Introduction

The Gulf of Alaska (GOA) is a semi-enclosed basin in the North Pacific Ocean, bounded by the mountainous coast of Alaska to the west, north and east, and open to the south. The bottom topography is complex; the depth of basin shoals toward the north with many deep canyons intruding onto the continental shelf, and numerous bays and inlets intersecting the coast. The region is dominated by strong storms, whose frequency vary on monthly to decadal scales. The regional meteorology in turn impacts the ocean circulation and nutrient supply, which ultimately support the rich ecosystem that characterizes the GOA.

Two current systems dominate the circulation of the GOA, the subarctic gyre in the ocean basin and the Alaska Coastal Current (ACC) on the continental shelf (Fig. 1). The southern boundary of the subarctic gyre is the West Wind Drift, which

*Corresponding author. Tel.: +1-206-526-6453.
E-mail address: stabeno@pmel.noaa.gov (P.J. Stabeno).

0278-4343/$ - see front matter © 2004 Elsevier Ltd. All rights reserved.
doi:10.1016/j.csr.2004.02.007

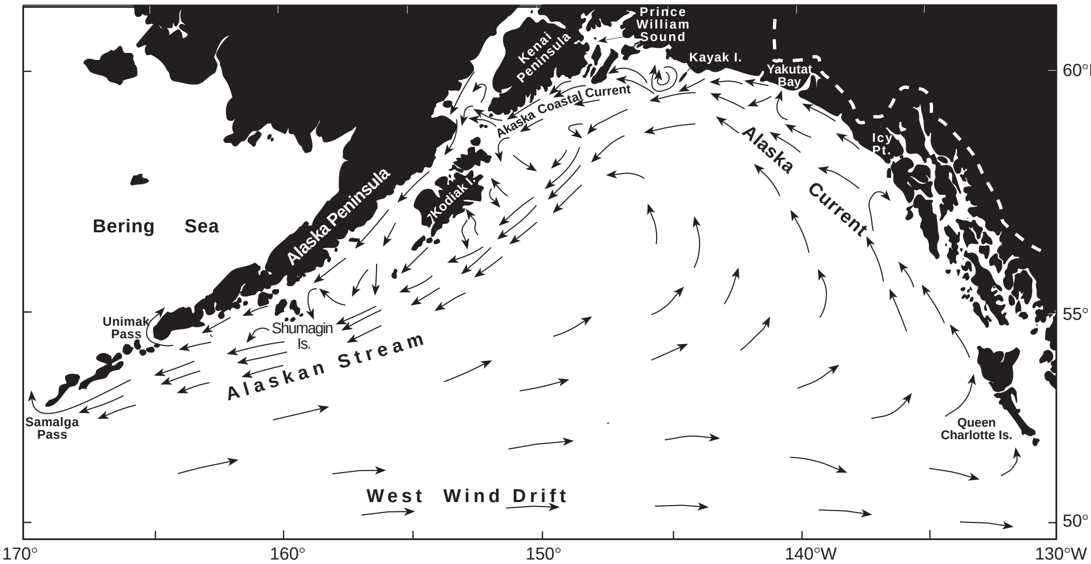

Fig. 1. Map of the Gulf of Alaska. The flow of the Alaska Coastal Current and subarctic gyre are indicated as are several geographic place names. (After Reed and Schumacher, 1986).

divides as it approaches the west coast of North America into the southward flowing California Current and the northward flowing Alaska Current. The Alaska Current is a typical eastern boundary current, rich with eddies and meanders. At the head of the GOA, it turns southwestward following the isobaths. This is the beginning of the Alaskan Stream, the western boundary current of the eastern subarctic gyre. Near the southwestern edge of Kodiak Island ($\sim 155°$W), the Alaskan Stream is a narrow (~ 50 km), high speed ($> 50\,\mathrm{cm\,s^{-1}}$) current that flows southwestward along the slope of the Alaska Peninsula and Aleutian Islands to 180°W, where the Aleutian Arc turns northwestward (Reed and Stabeno, 1989; Reed, 1984).

The ACC, driven by winds and freshwater runoff, dominates circulation of the shelf and controls the transport of dissolved substances and planktonic material (Stabeno et al., 1995a, b; Royer, 1981). While much is known through drifter trajectories and current meter moorings about the continuity, seasonal variability and mean flow of the ACC from the Seward Line ($\sim 149°$W) westward, less is known in the region south and east of Prince William Sound. Observations from Icy Point ($\sim 137°$W; Fig. 2) to Kayak Island reveal a baroclinic current with a strong seasonal signal in the freshwater core typical of the ACC farther west (Hayes and Schumacher, 1976). The ACC flows westward along the Kenai Peninsula and bifurcates at Kennedy-Stevenson Entrance with the majority of annual transport continuing down Shelikof Strait (Stabeno et al., 1995a, b; Schumacher et al., 1989). Approximately 70% of the transport continues down the Shelikof Sea Valley with less than half joining the Alaskan Stream, the remainder flows along Alaska Peninsula to Unimak Pass, and Samalga Pass, the western terminus of the ACC (Schumacher et al., 1989).

The continental shelf of the GOA supports a productive ecosystem, which includes numerous species of fishes, marine mammals and sea birds. The larvae of many species of vertebrates and invertebrates occur in surface waters. For many larvae, the ACC is their main path of dispersal. Coastal waters also provide a conduit for young salmon upon entering the oceanic environment. At first impression, such high productivity is surprising because GOA coastal winds are downwelling favorable. However, other mechanisms such as eddies and advection in canyons may replenish

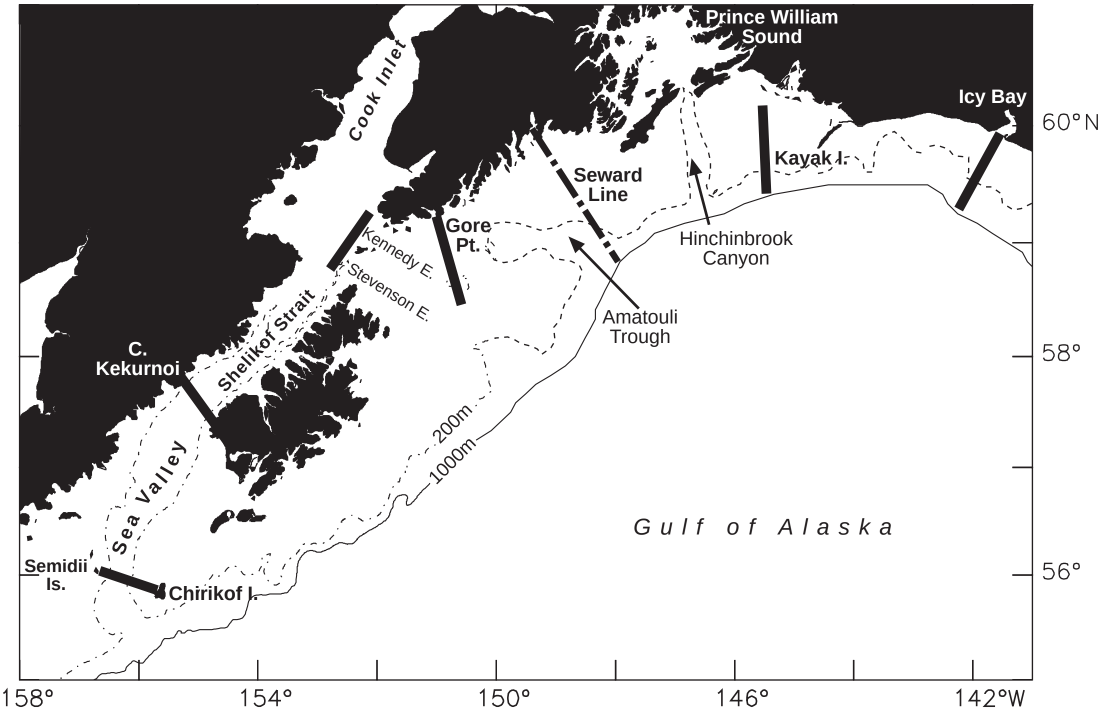

Fig. 2. Geographic place names and the locations of hydrographic sections (solid black lines) discussed in the paper. The Seward line is shown as a dashed line.

nutrients to the shelf and support this rich ecosystem. Global warming, decadal variability patterns (Pacific Decadal Oscillation: PDO; Pacific North American: PNA), El Niño-Southern Oscillation (ENSO) and large interannual variability all impact the ecosystem through changes in freshwater flux, water temperatures and regional winds (Hare and Mantua, 2000; Whitney et al., 1999). Changes in the physical system influence not only the supply of nutrients to the shelf, but also larval dispersal, and the timing and extent of phytoplankton blooms (Hermann et al., 1996; Stabeno et al., 1996; Napp et al., 1996).

In this paper, we integrate the knowledge about the ACC from Icy Bay along the shelf to its end in the eastern Aleutian Passes. While many papers have been published that focus on parts (i.e., along the Kenai Peninsula, Shelikof Strait, etc.) of the ACC, few exist that treat the system as a whole (Reed and Schumacher, 1986; Royer, 1998). Our purpose is to bring together historical and new information on the ACC that permits us to explore possible mechanisms generating cross- and along-shelf flow, and to provide a basis for future research.

The length of the coast and the varying mountainous terrain around the coastal GOA result in large spatial variability in the atmospheric forcing (wind and precipitation). This forcing, together with the complex bathymetry, results in changing oceanographic conditions around the perimeter of the GOA. To investigate these conditions, we first examine atmospheric forcing, including variability on seasonal to interannual time scales, in three regions (near Yakutat, the Kenai Peninsula, and the Shumagin Islands). This is followed by a review and update of the freshwater input along the Alaska Coast, in particular its spatial and temporal variability and chemical constituency. Next, we examine the oceanography (physics through primary production) of the ACC at three locations (near Kayak Island, Kenai Peninsula and Shelikof Strait).

Finally, we integrate the results with a focus on the mechanisms that result in the cross-shelf flux of nutrients and salts.

2. The atmosphere

The atmospheric forcing of the GOA is dominated by the effects of cyclonic storm systems. Their cumulative precipitation is the principal cause of the upper ocean's baroclinicity in the coastal zone, and their winds are a primary contributor to the local ocean circulation. Previous summaries of the meteorology of the GOA are provided by Wilson and Overland (1986) and Royer (1998). We include a brief review of the weather of the GOA as background for the primary objective of this section, the presentation of time series of coastal wind forcing.

The GOA is the terminus of the Pacific storm track. Even though these storm systems are generally in the latter stages of their lifecycles, they are so prevalent that the Gulf experiences mean wind speeds and frequency of gale-force winds similar to that of the western and central North Pacific (US Navy Marine Climatic Atlas, 1969). Storms tend to linger, while slowly spinning down, largely due to the coastal mountains bordering the Gulf (e.g., Wilson and Overland, 1986). This terrain inhibits the eastward progression of the storms, can intensify the winds, and causes large amounts of precipitation in coastal watersheds. The individual storms that constitute the atmospheric forcing have characteristic time scales of a few days, while their frequency and intensity vary on time scales of weeks to decades.

The weather of the GOA includes a pronounced, if not sharply defined, seasonal cycle. There is a strong tendency for the winds in the Gulf to be cyclonic during fall through spring, with a broad peak in storminess from October through March. These winds result in systematic upward Ekman pumping in the central GOA (Reed, 1984), and downwelling along the coast. The stronger of these storms, which result in most of the deepening of the ocean mixed layer, occur during the cool season. During May through September, the winds are variable, with cyclonic systems of weak to moderate intensity interspersed with periods of high sea level barometric pressure. The latter periods are accompanied by anticyclonic winds, and cause intermittent upwelling along the coast. These upwelling events, in particular the interannual fluctuations in their character, are elaborated upon below.

The seasonal variability in precipitation in the coastal GOA (as observed at three coastal weather stations; Fig. 3a) features a prominent wet period from September through November, and a minor, relatively dry period in June and July. Examination of the limited number of direct observations, together with those from satellites, of precipitation in the central GOA suggest that the annual mean precipitation in the central Gulf is about half of the 240 cm of water estimated to fall in coastal watersheds (Royer, 1979; Spencer, 1993). Because precipitation falls in the form of snow during winter and rain in the summer, which melts the snow and ice in coastal watersheds, the coastal

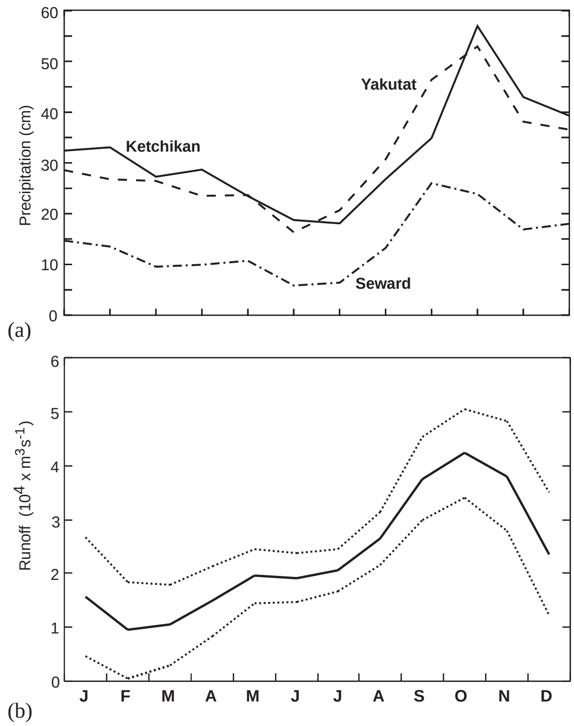

Fig. 3. The seasonal signal of (a) precipitation and (b) runoff along the Gulf of Alaska coastline. The lower panel is after Royer (1982) and dashed lines are ± one standard deviation.

GOA experiences a stronger seasonal signal in runoff than in precipitation (Fig. 3b). As estimated by Royer (1982), this runoff features an annual cycle with a peak in October of approximately $4 \times 10^4\,m^3\,s^{-1}$, and a minimum in February of approximately $1 \times 10^4\,m^3\,s^{-1}$. The freshwater or baroclinic contribution to the transport of the ACC leads the maximum local wind forcing by about 3 months (Royer, 1998). The annual freshwater discharge into the GOA of $\sim 2.4 \times 10^4\,m^3\,s^{-1}$ is comparable to that of the Mississippi River, $\sim 2 \times 10^4\,m^3\,s^{-1}$ (Dinnel and Wiseman, 1986).

2.1. Interannual to decadal scales

There is a growing appreciation that interdecadal variability in the atmosphere strongly influences the physical and biological systems of the North Pacific (Ingraham et al., 1998; Mantua et al., 1997; Francis and Hare, 1994; Hare and Mantua, 2000). Much of this variability can be attributed to a few fundamental patterns or modes. In general, much more attention has been paid to describing the decadal variability for winter than for summer. The leading contribution to the regional atmospheric variability in winter is the Pacific North American or PNA (Wallace and Gutzler, 1981; Barnston and Livezey, 1986). This mode relates to the strength and position of the Aleutian low (and hence wind, temperature and precipitation anomalies) over the GOA. Variations in the PNA, through its influence on surface fluxes of heat and momentum, are coupled to the PNA's counterpart in the ocean, the Pacific Decadal Oscillation (PDO; Wallace et al., 1992; Wallace, 2000).

On 3- to 7-year time scales, El Niño-Southern Oscillation (ENSO) can be an important influence on the GOA. El Niño events are typically accompanied by positive anomalies in wintertime air temperature, precipitation, along-shore wind (i.e., downwelling favorable) and sea level. La Niña periods tend to include anomalies in the opposite sense. When the ENSO cycle is relatively weak, other sources of variability intrinsic to the extratropical circulation dominate on interannual scales.

On decadal time scales, the PDO (Mantua et al., 1997) is the leading mode of North Pacific variability. The PDO features strong coupling between anomalies in sea surface temperature (SST) and sea level pressure (SLP) in the west-central North Pacific, with a secondary expression in the GOA. The atmospheric circulation anomalies associated with the PDO in the GOA resemble those for ENSO and it is unclear how much these two sources of variability are separable (Zhang et al., 1997). In discussing decadal variability, however, it is important to note that less than 38% of the wintertime interannual variance of the Aleutian low is on time scales greater than 5 years (Overland et al., 1999a). The primary east-west pattern of spatial variability of the PNA in winter, gives way to the more north–south dipole in spring, referred to as the North Pacific Pattern (Barnston and Livezey, 1986; Overland et al., 2002). Less is known about the causes of coastal GOA summertime variability, but it is expected that the key variables are the amount of cloud coverage, hence solar heating of the surface mixed layer (Norris et al., 1998), the frequency and magnitude of coastal upwelling events, and the occurrence of storms which impact both mixed layer depth and the strength of the ACC.

While these large-scale linkages between the ocean and atmosphere are reasonably well established for the North Pacific as a whole, it is still unclear how the large-scale atmosphere-ocean climate system relates to the coastal zone along the GOA. Essentially, a different set of "rules" applies to air–sea interactions in this region because of the presence of the mountainous coastal terrain. This terrain is particularly important through its impact on the along-shore winds, which forces cross-shelf Ekman transports, and precipitation, which impacts the upper ocean's baroclinicity. Relatively subtle differences in the large-scale atmospheric flow (e.g., low-level static stability and wind direction) can result in substantial differences in the atmospheric response to the coastal terrain. Without further study, we cannot relate important mechanisms involving the ACC, such as the timing of seasonal reversals in the normally downwelling-favorable winds, to the large-scale variations in the climate forcing. Yet it is these downscale effects of climate variations that are liable to be crucial to the ACC, and to the marine ecosystem in the coastal GOA.

2.2. Winds

Air–sea interaction mechanisms important to the coastal GOA are presented below. The focus is on time series of seasonal mean along-shore winds and wind mixing in the cool season, and upwelling in the summer. The analysis consists of time series at selected points along the coast. These results are not so much definitive, as illustrative of the interactions between wind and buoyancy on upper ocean in the coastal GOA, and are related to the forcing of physical oceanographic observations noted in later sections.

The coastal winds are estimated using daily data from the NCEP/NCAR Reanalysis (Kalnay et al., 1996) with a simple correction for the effects of coastal terrain on nearshore winds. This correction was arrived at through comparisons between synthetic aperture radar (SAR) estimates of the winds (as provided by Johns Hopkins University Applied Physics Laboratory; see /manati.wwb.noaa.gov/sar_pub_5s/ APL_winds/wind_images/index.html) with those from the Reanalysis for the cool season of 1999–2000 and the warm season of 2000, at selected locations along the coastal GOA. The wind speeds from SAR averaged about 50% higher than those estimated from the Reanalysis during periods of positive (southerly or easterly) along-shore winds (i.e., with the terrain on the right) but were similar in magnitude during conditions of negative (westerly or northerly) along-shore winds. Similar enhancements were found at the different locations surveyed. Based on these results, we assumed that the along-shore component of the winds were 50% greater in magnitude than in the Reanalysis when positive, and equal in magnitude to that in the Reanalysis when negative. The component of the wind in the cross-shore direction was unchanged. We note that our correction is designed to account for the effects of coastal terrain in an average sense; these effects vary for individual storm events.

Enhancement of the low-level winds during periods of positive along-shore flow is expected due to the prominent terrain along the GOA. This phenomena is known as a barrier jet (e.g., Parish, 1982). The zone of stronger winds extends offshore approximately an atmospheric Rossby radius (50–100 km for the GOA). The magnitude of the enhancement found here is consistent with the results of Overland and Bond (1995), and with the wind algorithm used by Stabeno et al. (1995a, b) for forcing a numerical model for Shelikof Strait. These enhanced along-shore winds are present in the SAR data, but not captured in the Reanalysis because of the latter's coarse (2.5° latitude) resolution relative to the Rossby radius, and its consequent inability to resolve the effects of the coastal terrain. Inspection of individual cases from the Reanalysis also suggest that the direction of surface winds in the coastal zone are not parallel to the coast, as is generally observed.

The mean seasonal cycle in the coastal winds of the GOA is illustrated in Fig. 4. As mentioned earlier, the GOA is stormy during the cool season, and calmer during the warm season, but there are substantial regional differences. The seasonal cycle in storminess (as gauged by the wind speed cubed; Fig. 4c) is more prominent at the western location (55°N 160°W near the Shumagin Islands) than at the north-central and north-eastern locations. The mean cross-shore wind is weak through much of the year (Fig. 4a), although during early fall, winds at the north-eastern location are slightly onshore, while winds at the western location are more offshore. The mean along-shore wind is more positive at the north-eastern location than at the north-central and western locations throughout the year (Fig. 4b). The north-eastern location also experience a stronger seasonal signal in this component of the wind. The annual cycle in the coastal winds of the GOA has important consequences for the ACC (Royer, 1998; Stabeno et al., 1995a, b), but the interannual variability in the coastal forcing must also be considered.

The interannual variability in the seasonal mean forcing is examined next, focusing on the summer (June–August) with its intermittent upwelling-favorable winds, and the cool season (October–March) with its systematic downwelling-favorable winds. The mean along-shore wind, total upwelling, and mean wind speed cubed during summer for the years 1949 through 2000 at the same three coastal locations is shown in Fig. 5. We define the total upwelling to be the integrated along-shore wind stress (using the algorithm of Large and

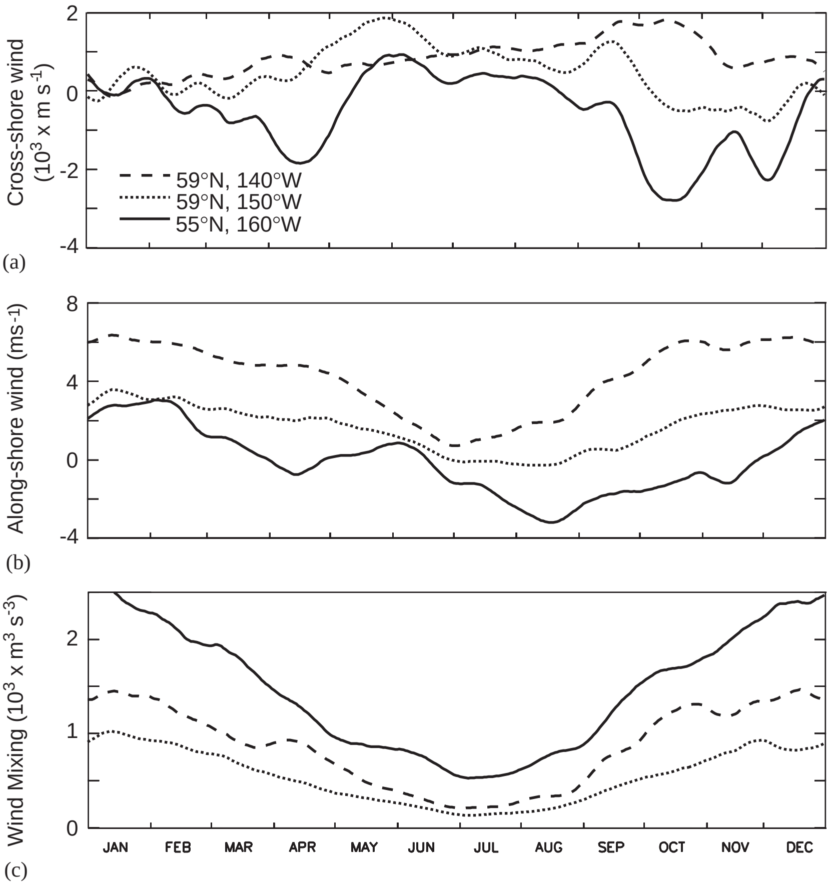

Fig. 4. The annual cycle in winds at selected locations: (a) the cross-shelf winds, (b) the along-shore winds, and (c) wind mixing (daily mean wind speed cubed). The annual signal was created from daily averages over a 52-years period (1949–2000).

Pond, 1982) considering only the periods of negative along-shore winds (i.e., upwelling favorable winds). It is the along-shore component of the stress that is related to the cross-shelf Ekman transport (e.g., Gill, 1982), and because the stress is nearly proportional to the square of the wind speed, this measure effectively accounts for the few strong events that produce most of the upwelling. Note that while the mean summer along-shore winds are only slightly more negative ($\sim 1\,\mathrm{m\,s^{-1}}$) at 55°N 160°W than at 59°N 150°W, the total upwelling at the former location tends to be about three times greater. A common characteristic of the time series shown in Fig. 5 is the lack of any discernible decadal signals or long-term trends. The year-to-year fluctuations are large, however, especially at the three southern locations, where typical anomalies are roughly 50% as large as their means. Alternatively, upwelling or mixing is typically three times greater in strong years relative to weak years. Such large interannual variability likely have important implications for the supply of nutrients to the euphotic zone over the shelf in the summer.

Next we consider the interannual variability in coastal wind forcing during the cool season. During this time of year, the wind mixing is usually vigorous and the surface heat fluxes to the atmosphere are substantial, resulting in a relatively well-mixed water column. The most important aspect of the coastal winds is their along-shore component, which regulates the transport of the ACC (Stabeno et al., 1995a, b). We include time series of seasonal mean in the along-shore wind

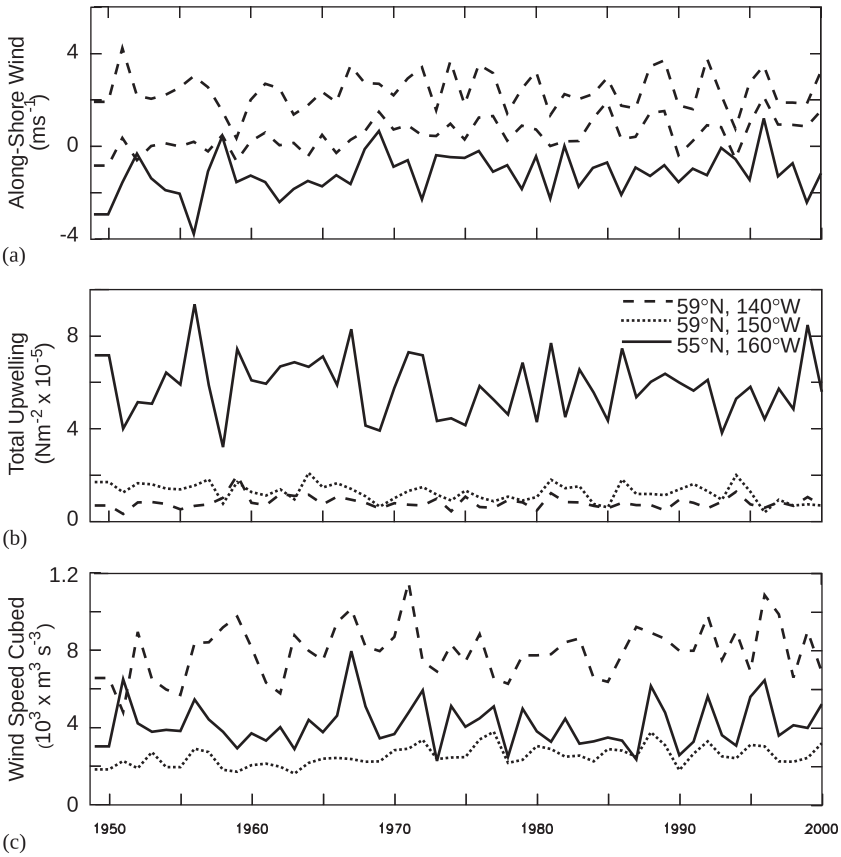

Fig. 5. The summer (a) mean along-shore wind, (b) total upwelling, and (c) mean wind speed cubed for the years 1949 through 2000 at the three coastal locations discussed in the paper.

speed and the wind stress. The former has often been compared to along-shore transports in coastal regions but the latter is related more directly to the cross-shore component of the Ekman transport and hence the set-up responsible for the barotropic portion of the coastal flow. These two measures are obviously highly correlated but there are some interesting differences. Notably, the average stress at the western most location (55°N, 160°W) is negative even though the average along-shore wind is positive, consistent with the tendency for stronger, but less frequent, winds to be from the west rather than from the east. Also, the winds in the northeastern GOA are almost always more positive than their counterparts in the north-central and western GOA.

Similar to the summer winds, the winter winds exhibit considerable interannual variability. Interestingly, any clear signature of the PDO (Mantua et al., 1997) and the regime shift in 1977 is lacking. There were largely negative seasonal mean wind speed and stress anomalies from the mid-1960s to mid-1970s, and positive anomalies from the late 1970s through 1980s, especially in the eastern GOA. But on the whole, the coastal winds do not reflect the PDO. This can be explained by noting that the winds relate to coastal SLP gradients, which are sensitive to the position and intensity of the Aleutian low, and the Aleutian low is impacted by factors other than the PDO (Overland et al., 1999a, b). The year-to-year, rather than decadal, variability in the coastal wind forcing in both winter and summer is substantial, and this likely

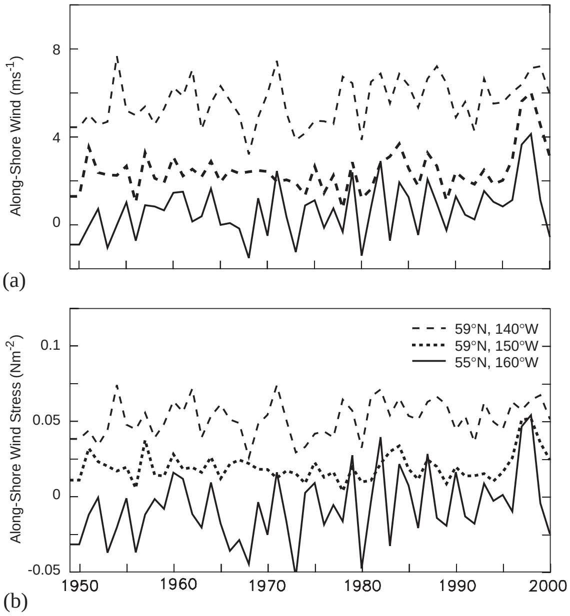

Fig. 6. The winter (a) mean along-shore wind, and (b) mean along-shore wind stress for the years 1949 through 2000 at the three coastal locations discussed in the paper.

has important implications for the year-to-year variability in the ACC (Figs. 5 and 6).

2.3. Rainfall and runoff

Runoff is crucial to the baroclinic structure of the ACC. We focus on the interannual variability in precipitation and air temperature, which together control the magnitude and timing of the freshwater input to the ACC, and concentrate on the northern and eastern portions of the GOA, where most of the freshwater for the ACC originates. We use observations of precipitation and temperature from coastal weather stations, rather than the NCEP Reanalysis data set that was used to estimate coastal winds. The Reanalysis likely includes much greater errors in precipitation than surface winds, since the precipitation is effectively a higher-derived quantity than the wind and less constrained by observations. Virtually no long-term precipitation records are available above sea level in the GOA's watersheds, so the records presented below should be considered indices, rather than absolute measures of the freshwater input. As in the discussion of winds, we consider the cool and warm seasons separately.

Time series of total precipitation and mean air temperature at Ketchikan, Yakutat, and Seward for the warm seasons (defined as May through October following Royer, 1979) of 1950 through 2000 are plotted in Fig. 7. Apart from year-to-year variability, little if any systematic signal is apparent in either precipitation or air temperature. One exception is the relatively wet conditions at Yakutat from the late 1980s through the early 1990s, but it is uncertain how important this is since the other two stations did not experience sustained anomalies. In the warm season, the precipitation lacks any significant systematic relationship with air temperature and is at best weakly related to the coastal winds with correlation coefficients less than 0.11 at all three stations.

The time series of precipitation and air temperature during the cool season (November through April) show greater interannual variability than that during the warm season, and some decadal signals (Fig. 8). The major PDO regime shift of 1977 was accompanied by a transition to slightly wetter conditions at Yakutat and Seward, and perhaps slightly drier conditions at Ketchikan. The regime shift is even more evident in the air temperature at Yakutat and Seward, which experienced colder winters in the late 1960s and early 1970s, followed by warmer winters in the late 1970s and 1980s. As mentioned earlier, it is uncertain how to quantify the causes of this decadal change because of the possible interactions between the PDO and ENSO. It is noteworthy that the El Niños of 1977, 1987, and 1998 all featured warmer, wetter winters in the northern GOA.

Unlike the warm season, precipitation and mean air temperature during the cool season are positively correlated in the northern GOA. The correlation coefficients between the along-shore winds and the coastal precipitation are 0.29, 0.28, and 0.21 at Ketchikan, Yakutat, and Seward, respectively. While these values are modest, they are significantly different from zero at the 95% confidence level. The typical magnitude of the temperature anomalies is 2°C, which corresponds to anomalies in the freezing level of $\sim$300 m. This has important consequences for runoff. Cool

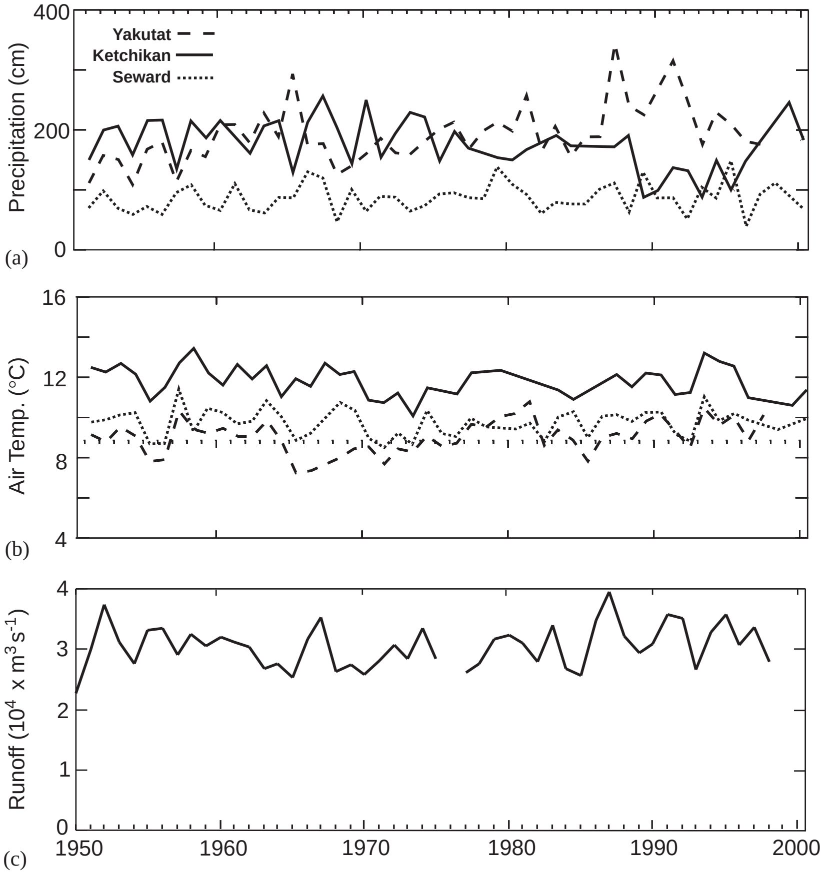

Fig. 7. Time series of the average (a) total precipitation, (b) mean air temperature at Ketchikan, Yakutat, and Seward during the warm seasons of 1950 through 2000. The warm season is defined as May through October following Royer (1979). The average runoff for the Gulf of Alaska for June through November (1950–2000) is shown (c).

winters may result in an enhanced snow pack, and thus a possible increase in runoff during the warm season. Warm winters will tend to have significantly enhanced runoff not just because of greater precipitation, but also because the snow/ice line will be higher in elevation and farther north than usual. The technique used by Royer (1979), in which a constant fraction of the coastal precipitation in winter is assumed to be runoff, may lead to significant errors. There does not seem, however, to be any straightforward way to assess this temperature effect, since so few of the coastal GOA rivers are gauged. The implication for the ACC is that wet winters, with their enhanced upper ocean baroclinicity, also tend to include a greater wind forcing of the barotropic component.

A strong seasonal signal exists in the freshwater discharge time series (Fig. 3) that was developed by Royer (1982), which includes a factor based on temperature. Minimum runoff occurs during the cold winter months and maximum runoff occurs in early fall, when precipitation increases, and temperatures remain above freezing (Fig. 3b). We divided the runoff into two parts: high (June–November) and low (December–May), which are shifted 1 month later than the monthly averaged precipitation and temperature time series (Figs. 7a,b and 8a,b). During June–November, runoff is approximately double that during December–May, and the variability is slightly less (Fig. 7c and 8c). Decadal variability is not clearly evident in either time series, although analysis by Royer

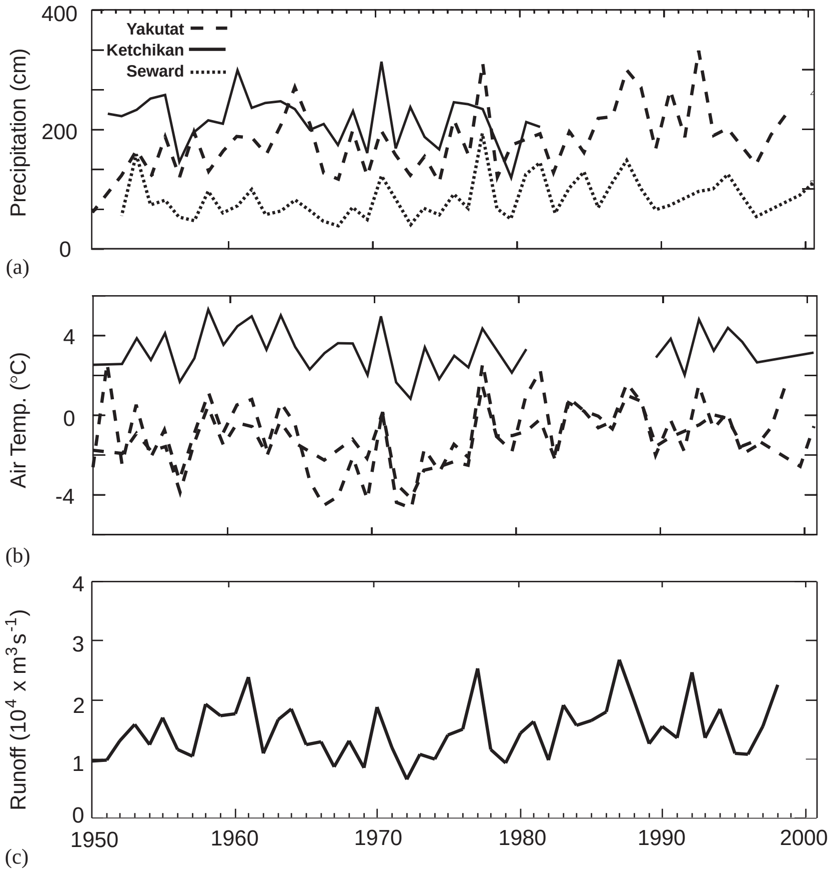

Fig. 8. Time series of average (a) total precipitation, (b) mean air temperature at Ketchikan, Yakutat, and Seward during the cold season of 1950 through 2000. The cold seasons is defined as November through April. The runoff for the Gulf of Alaska for December through May for each year (1950–2000) is also shown (c).

and Grosch (2000) shows that approximately a quarter of the variability is in a pair of bands centered on 15 and 42 years. As expected since the time series of freshwater discharge is derived from atmospheric variables, years of high runoff during winter and spring (i.e., 1978) are associated with years of above average temperatures during the cold season and high precipitation. The weaker runoffs during winter/spring (i.e., 1972) are associated with colder than average temperature and not as sensitive to precipitation. The summer-fall runoff is related predominately to rainfall, with temperatures warm enough to play little role in variability.

In addition to the flux of freshwater, coastal runoff contributes nutrients necessary for phytoplankton production. The riverine contribution may be especially important in summer when runoff is near the seasonal maximum and surface concentrations of nutrients over the shelf are otherwise depleted (discussed below). However, as noted by Sugai and Burrell (1984) and Burrell (1987), nutrient levels likely vary depending on the freshwater source (e.g., glacial vs. non-glacial, rivers with varying freshwater residence times). In addition, sediment discharge in fall can dramatically reduce the photic zone and dampen fall blooms (Goering et al., 1973; Burrell, 1987). Riverine discharge adds significant iron and silicic acid to the ACC. Dissolved iron and silicic acid concentrations average about 3 and 100 μM, respectively, for drainage basins throughout southern Alaska (Glass, 1999; USGS Web Page, Marc

Kramer, pers. comm.). During summer, the ACC east of Cook Inlet is about ~8% fresher, indicating a contribution of about 8 μM silicic acid to the ACC from freshwater sources. The flux of nitrate from riverine sources is unclear. Organically rich streams may be severely N limited such that any available NO_3^- is rapidly taken up and is undetectable (M. Kramer, pers. comm.). Other studies found relatively high nitrate concentrations near river inputs at Port Valdez (15 μM; Goering et al., 1973) and from several rivers entering Smeaton Bay in southeast Alaska (2–6 μM; Sugai and Burrell, 1984). Average "nitrate plus nitrite" concentrations in USGS water quality studies were about 13 μM. Hence, given typical freshening observed in the ACC, freshwater discharge only adds about 1 μM nitrate to surface waters of the ACC.

3. Oceanography

In comparison to the meteorological data, oceanographic data for the GOA are limited. Only through combining historical data from hydrographic cruises, instruments on moorings, satellite-tracked drifters and satellite images have we been able to develop a picture of ocean conditions in the GOA. These data sets, coupled with modeling results, permit the characterization of the currents and water properties of the region.

A coastal current with a marked freshwater core is evident along the Alaska coast from Icy Point to Unimak Pass (Stabeno et al., 2002; Schumacher et al., 1982). Along its course, it is modified by both broad scale cross-shelf Ekman transport and episodic entrainment from the slope, as well as by topographic steering at a variety of sites, including Kayak Island, Hinchinbrook Canyon and Amatouli Trough. The large freshwater discharge from numerous rivers and streams along the mountainous Alaska coastline is confined along the coast by downwelling favorable winds. This combination provides a strong baroclinic signal to the ACC. In response to variations of wind forcing and buoyancy flux, maxima in along-shore transport can exceed $3.0 \times 10^6\,m^3\,s^{-1}$ (e.g., Stabeno et al., 1995a, b; Stabeno and Hermann, 1996; Bond and Stabeno, 1998) and daily averaged speeds can exceed $100\,cm\,s^{-1}$ (Stabeno et al., 1995a, b; Royer, 1998). The transport in the ACC varies on seasonal time scales with maximum baroclinic flow occurring in October in conjunction with maximum freshwater runoff; maximum total transport (as measured from current meter moorings) is in the winter and associated with the strong winter winds (Schumacher et al., 1989).

The complexity of the ACC over the shelf is evident in a series of chlorophyll images taken in the spring of 1997, 1998 and 1999 (Fig. 9). Detailed spatial structures are apparent in the chlorophyll-*a* distributions provided by SeaWiFs and ADIOS. It is uncertain how much of the patchiness in these chlorophyll distributions relates to physical processes such as localized upwelling and eddies, versus biological processes such as grazing.

3.1. Lagrangian measurements

Lagrangian devices or drifters provide information on the spatial characteristics (such as eddies, bifurcation and meanders) in the ACC, locations of onshelf flow and mean circulation. Over 100 satellite-tracked drifters have been deployed in the GOA during the last 15 years. Most were deployed west of Prince William Sound. Typically the drogues were at 35–45 m, so that direct effects of wind and wind-wave generated currents were small, and the ensuing trajectories provide a description of the underlying oceanic current structure. A description of data control and accuracy of these instruments is found in Stabeno and Reed (1991).

A general description of the flow in the ACC from Kayak Island to Unimak Pass can be made using drifter trajectories. Approximately a dozen satellite-tracked drifters were deployed between Icy Point and Kayak Island in 2001 and 2002. While an organized flow is evident along the coast between Icy Point and Kayak Island, during summer most of the drifters were diverted to the shelf break at Kayak Island (Fig. 10a). Only one drifter was advected into Prince William Sound. Drifters deployed along the Seward Line (~149°W, Fig. 10b) reveal episodic across shelf flow and a relatively unorganized ACC. The drifters in Fig. 10b were deployed in May 2001,

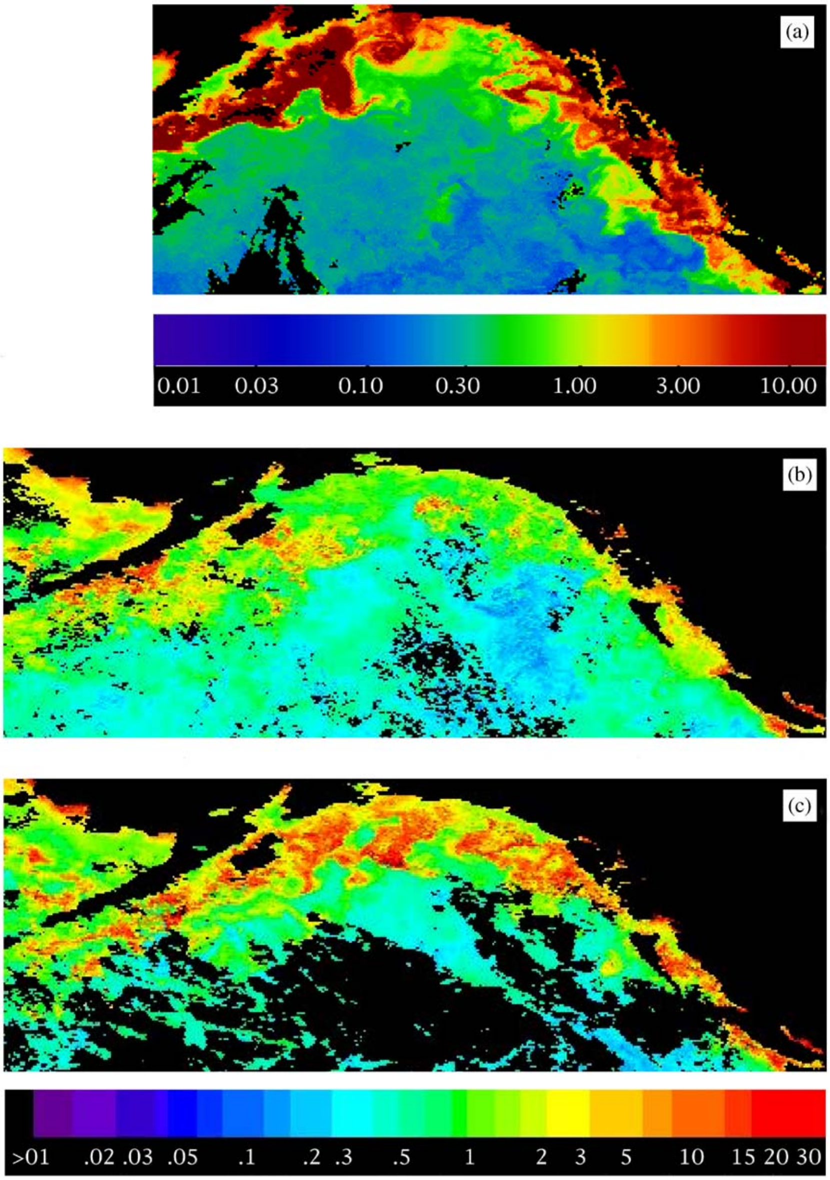

Fig. 9. Satellite images of chlorophyll-*a* from (a) May 18–24 (ADEOS), (b) May 1998 (SeaWiFs), and (c) June 1999 (SeaWiFs). Both the land and clouds are black. Note the different scales for ADEOS and SeaWiFs (from Whitney and Welch, 2001).

and the effects of weak winds that characterize the warm season are evident in the trajectories. As the drifters approached Gore Point the current becomes more organized. The ACC bifurcates as indicated by drifter trajectories; one drifter (green) entered Shelikof Strait through Kennedy Entrance and the other (dark blue) was advected along the south-west side of Kodiak Island (Fig. 10c). Such flow patterns are relatively common in drifter trajectories (Fig. 10d). The flow along the south side of Kodiak is relatively weak and variable, while the flow in Shelikof Strait is stronger, and largely centered on the north side of the strait. Upon exiting Shelikof Strait, meanders once again

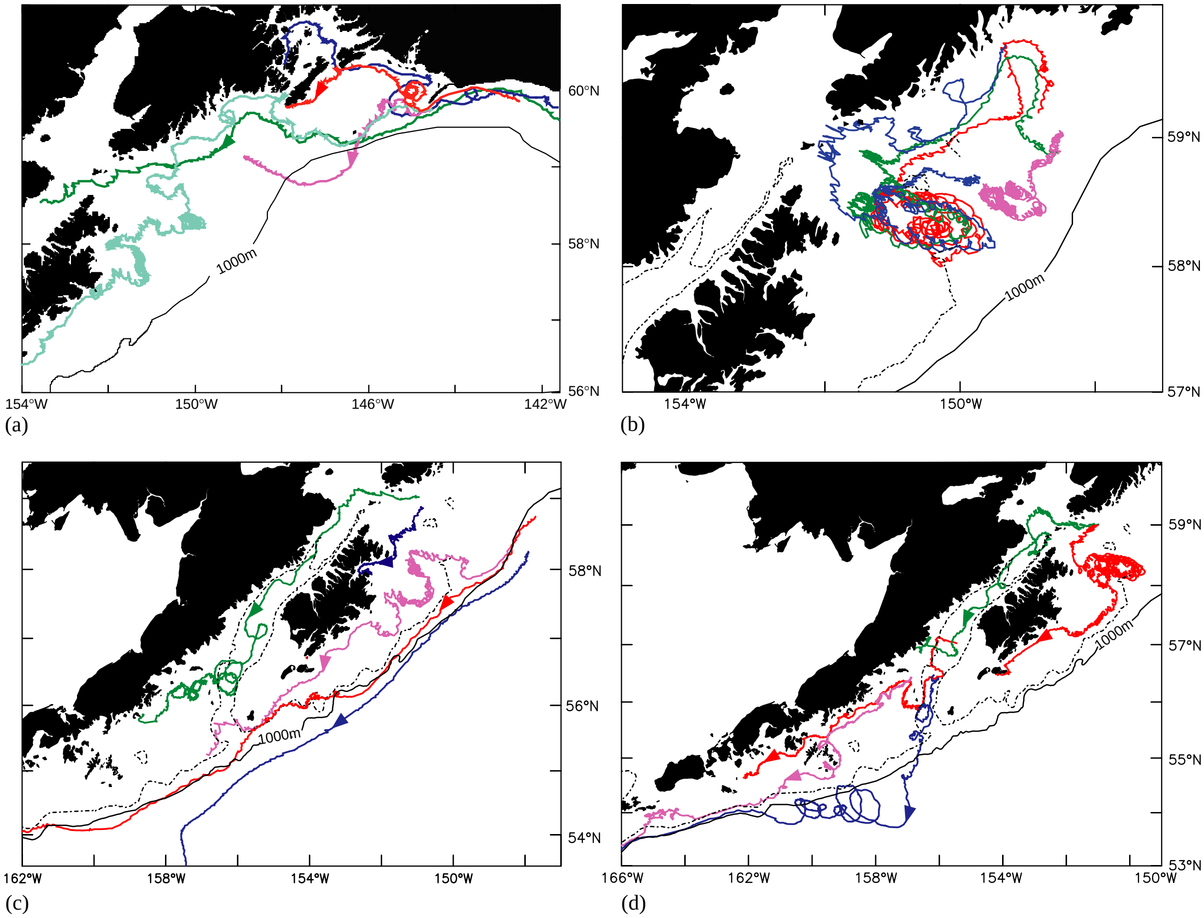

Fig. 10. Trajectories of satellite tracked drifters (depth of drogue ~40 m). The arrows indicate the direction of flow. The small loops on the trajectories are tidal motion. (a) Flow along the shelf. Only one drifter deployed east of Kayak Island was advected in Prince William Sound. (b) Convoluted flow along the Kenai Peninsula, (c) trajectories on each side of Kodiak Island with a retention area over Portlock Banks, and (d) drifters west of Shelikof Strait.

became more prominent, although not to the extent that was observed along the Kenai Peninsula. Eddies (diameter 20–30 km, depth 200 m; green in Fig. 10c) are also evident in the sea valley southwest of Kodiak Island, and drifters have remained trapped in such features for several weeks (Bograd et al., 1994; Schumacher et al., 1993). Most of the flow of the ACC continues down the sea valley (blue, Fig. 10d), although some parallels the Alaska Peninsula (purple, Fig. 10d). The transport in the sea valley exits the shelf and joins the Alaskan Stream, or recirculates onto the shallow shelf west of the sea valley. The flow along the peninsula continues westward through or around the Shumagin Islands. Some drifters enter the Bering Sea through Unimak Pass (Stabeno et al., 2002); others join the Alaskan Stream (Fig. 10d). The exact percentage of transport that goes with each path is not known and would be best estimated from an array of current meter moorings.

Flow along the shelf break and slope is more organized than that on the shelf, with the Alaskan Stream evident in trajectories. Of three drifters deployed along the slope (water depths 1000–2000 m), one (purple, Fig. 10b) was advected onto the shelf. A second drifter (red) was also advected onto the shelf and followed the 200 m isobath, until rejoining the Alaskan Stream at the mouth of the Shelikof sea valley. The third drifter (blue) remained in the Stream until it was advected into the basin at about 158°W. Eddies in the stream are not uncommon (e.g., Fig. 10d, blue).

Results from a numerical model (details of model can be found in Hermann et al., 2002), show the complexity of current along the shelf from east of Kayak Island to Shelikof Strait (Fig. 11). The Alaska Current and Alaskan Stream are evident along the slope. The narrowness of the shelf east of grid point 126 results in the Alaska Current interacting with the shelf flow. Unfortunately, the coarseness of the model grid was such that Kayak Island was not resolved. To the east of Prince William Sound, two eddies are apparent; such eddies are also evident in some satellite-tracked drifter trajectories (Fig. 10a). On shelf flow occurs in the vicinity of the Seward line, which is also in agreement with the satellite-tracked drifter trajectories. Finally, the flow narrows at Gore Point and then passes through Kennedy Entrance. In general, there is good agreement between the currents predicted by the model and those derived from satellite-tracked drifter trajectories.

3.2. Time series from moorings

Moorings have been deployed on the GOA shelf since 1974 and these mooring sites can be divided into three general areas. In the eastern region (Kayak) extends from Icy Bay west to Kayak Island, moorings were deployed year around at ten sites from 1974 through 1976 (Hayes, 1979). The second region (Kenai) extends along the Kenai Peninsula and into upper Shelikof Strait. Moorings were deployed in a line across the shelf at Gore Point in 1991 and 1994, and in Kennedy and Stevens Entrances in 1991 (Stabeno et al., 1995a, b). Moorings have been deployed as part of GLOBEC on the Seward Line, but those data are not yet available. The third region (Shelikof) extends from the western exit of the Shelikof Strait west to the Shumagin Islands. Over 70 moorings have been deployed in Shelikof sea valley and the shelf to the east since 1984; the majority of these time series are during spring and summer. Unfortunately, there is little overlap in time between the three regions. All moorings were taut wire moorings that recorded hourly or half-hourly data. Instrumentation and mooring designs can

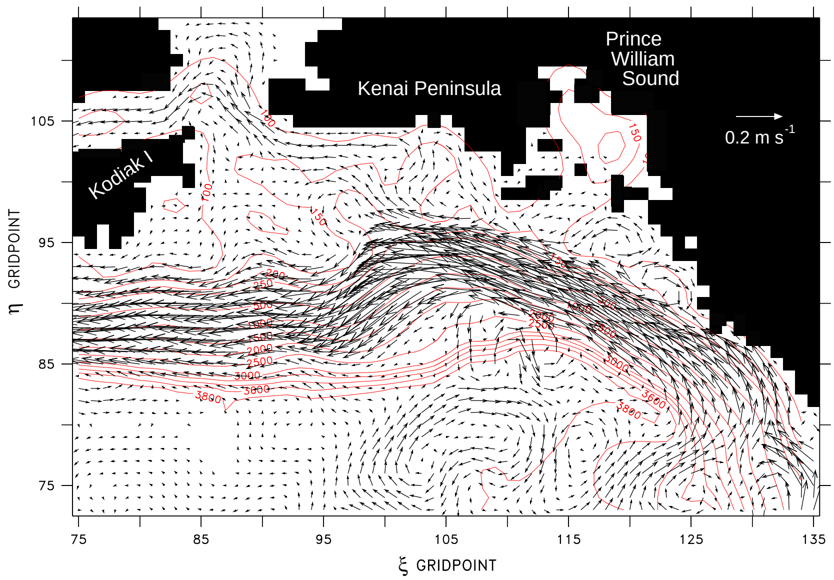

Fig. 11. Depth integrated current velocities from a model (Hermann et al., 2002). The coast has been rotated, ~45° counterclockwise. The red lines indicate bathymetry in meters. Vectors are in m s^{-1}.

be found in a variety of publications (Schumacher et al., 1989; Stabeno et al., 1995a; Hayes, 1979; Hayes and Schumacher, 1976).

3.2.1. Tidal currents

Tidal analysis of each of the time series provide a map of the variability in strength and direction of the tidal constituents along the shelf. The dominant tidal component in each region is M_2. The axis of the tidal ellipses parallels the coast with significant spatial variability along the coast. Beginning at Icy Bay, the tidal constituents are relatively weak with the amplitude of M_2 approximately 2–5 cm s^{-1}. To the west of Kayak Island, the M_2 tidal currents increase to 17 cm s^{-1} near the shore and ~10 cm s^{-1} at the shelf edge. At Gore Point M_2 has strengthened to 20–30 cm s^{-1}. The strongest measured tidal currents are in Kennedy Entrance, where M_2 is >70 cm s^{-1}. In the Shelikof region tidal velocities (20–30 cm s^{-1}) are similar to those at Gore Point.

3.2.2. Low-frequency currents

The width, speed and depth of the ACC varies with location along the coast. From Kayak Island west to Seward Line, the ACC is convoluted with significant mesoscale activity, likely due to the complex topography. At Gore Point, it narrows (~50 km wide) and flows westward parallel to the coast with few reversals on daily time scales. This more organized flow is likely a result of less complex topography. Gore Point lacks canyons cutting perpendicularly into the shelf, which are common along the eastern half of the Kenai Peninsula. In addition, Gore Point is farther removed from eddies that influence on-shelf transport. Farther down stream at Cape Kekurnoi, the ACC narrows to ~30 km wide, and then widens again as it flows down the Shelikof Sea valley.

Using data from the moorings, we examined the currents at a depth of 20–35 m at three locations along the continental shelf (Fig. 12). The current records were divided into three subsets: near coast, mid-shelf and outer shelf. Examination of alongshore currents reveals a seasonal signal in velocity, with a tendency for weaker currents during summer (May–August) and stronger currents during fall and winter, especially at Gore Point. East of Kayak Island, the current speed does not appear to be associated with cross-shelf position (Fig. 12a). The strongest current was often near the middle of the shelf or even at the outer edge. At Gore Point (Fig. 12b), the highest speeds are near the coast, and decrease monotonically with distance from the coast. In Shelikof Strait (Fig. 12c), the strongest currents are along the Alaska Peninsula, where some individual monthly means exceeded 50 cm s^{-1}. The currents are weaker near the middle of Shelikof Strait and along Kodiak Island, where currents often reverse. While a seasonal signal is not evident in the flow along the peninsula, the speed nearest the center of the strait appears weakest in the summer.

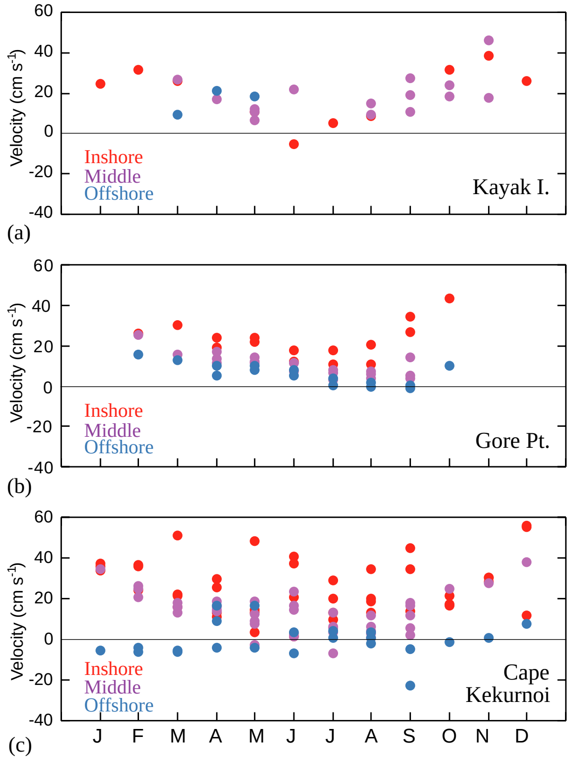

Fig. 12. Time series of monthly mean near surface currents at three locations (east of Kayak Island, Gore Point and Cape Kekurnoi) along the GOA coast. Red dots are velocity measured along the coast, purple at mid shelf and blue at outer shelf.

3.2.3. Relationship of currents to wind forcing

Correlations between winds and individual current meter records are generally not significant, due to the temporal variability in the position of the ACC on the shelf and the presence of meanders and eddies. Two locations where correlations between winds and currents have been significant are to the east of Kayak Island (Hayes, 1979; Hayes and Schumacher, 1976) and along the Alaska Peninsula in Shelikof Strait (Stabeno et al., 1995a). The strong ageostrophic winds that accelerate down Shelikof Strait result in a narrow current confined along the coast (Lackmann and Overland, 1989; Bond and Stabeno, 1998; Stabeno et al., 1995a, b). A better indication of how winds relate to the ACC is through an examination of transport (derived from current meters) and wind forcing. During four different years (1984–1985, 1989, 1991, and 1996), there were sufficient moorings deployed to measure total transport of the ACC across Shelikof Strait or across the sea valley (Stabeno et al., 1995a; Bograd et al., 1994; Schumacher et al., 1989). The times series of currents used here were all low pass filtered to remove the tides.

During 1991, transport was calculated at Gore Point, Kennedy and Stevenson Entrance and at the exit to Shelikof Strait (Stabeno et al., 1995a). Correlations among transports were all significant. During periods of high transport, most of the flow at Gore Point flows down Shelikof Strait but during periods of weak transport a significant portion flows south of Kodiak Island (Stabeno et al., 1995a). Mean transport in Shelikof Strait during winter (October–April) was $\sim 1\times10^6\,m^3\,s^{-1}$, with transport ranging from $\sim 3.5\times10^6$ to $-0.5\times10^6\,m^3\,s^{-1}$ (Fig. 13). During summer, both the mean transport ($<0.5\times10^6\,m^3\,s^{-1}$) and the variability was less than during the winter.

The high variability observed in the transports appears related to the along-shore wind (6-hourly winds from the NCEP Reanalysis, at 59°N 150°W). Using the four time series of transport in Shelikof Strait and sea valley, we divided the transports into three subsets (January–April, May–August and September–December) to remove the annual signal (Fig. 14). For each subgroup, the transport lags the wind by 12 h. The correlations range from $r = 0.42$ during the fall, to $r = 0.54$ in the winter and early spring. Lower correlations with the wind in the fall may be in part due to the large freshwater input which may modify transport. The lower correlation in the summer likely results from the weaker wind forcing during this period.

Model simulations (Hermann and Stabeno, 1996) also show that while baroclinic structure is related to runoff, the transport is largely determined by winds. Doubling the magnitudes of the winds results in an increase in transport, however a doubling in the magnitude of the runoff does not result in a significant increase in transport. Along-shore, downwelling favorable winds are necessary to confine the freshwater discharge along the coast, which then results in the ACC. Without downwelling winds, the freshwater appears to pool at the fresh water source.

Conclusions about the variability in transport can be drawn from examination of along-shore winds. The year-to-year variability of the along-shore winds during winter in the northern GOA (Fig. 6) is not particularly large and thus the year-to-year variability in transport during winter is likely not large. Alternately, during summer (Fig. 5), there are years when the along-shore winds would support a more vigorous ACC. Biological productivity during the summer is

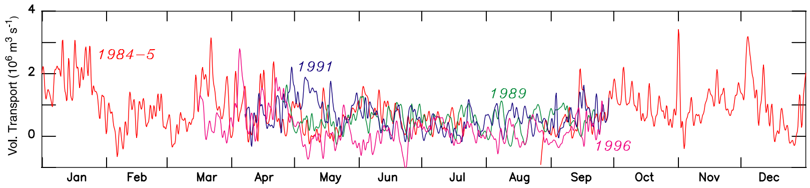

Fig. 13. Transport ($10^6\,m^3\,s^{-1}$) measured using current meters at Cape Kekurnoi (August 1984–January 1985, 1991, and 1996) and further down the sea valley (February–July 1985 and 1989).

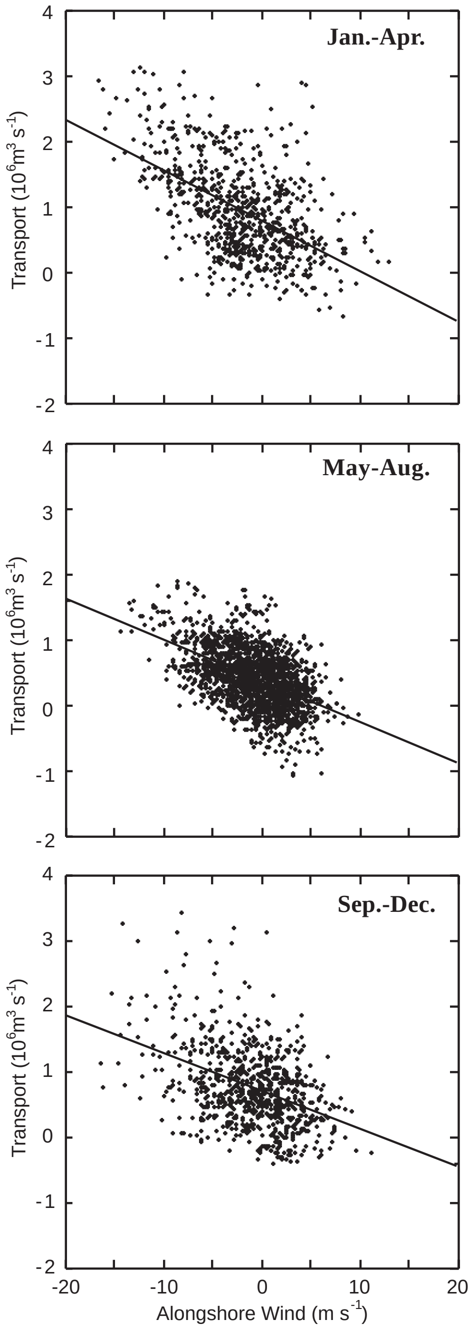

Fig. 14. Scatter plot of along-shore winds along the Kenai Peninsula versus transports shown in Fig. 13. The maximum correlations which occurred at 12 h lag are shown.

dependent upon available nutrients, and the variability in transport of the ACC would likely impact the availability of nutrients.

3.3. Hydrography

The cross-shelf hydrographic structure was examined at six locations during September and October and four locations during May (Fig. 2, Figs. 15 and 16). Evident in each section is the freshwater core of the ACC that is prominent in fall and less so in the spring. The easternmost location is at Icy Bay, where measurements extended into the bay. In the September 1977, Icy Bay salinity was below 26 psu. Even outside the bay, salinities were less than 30 psu, indicative of the strong freshwater influence of the ACC. At both Kayak Island and Gore Point, autumn salinities below 30 psu occur. Surface salinities beyond Kennedy Entrance, however, increased to above 31 psu and remained high into Shelikof Strait and the sea valley. Typically, the less saline water was confined along the coast in the upper part of the water column, with salinities above 32 psu evident below 100 m. Over the shelf, the highest salinities (>33.5 psu) were at Chirikof Island, where water drawn from the slope flows up the sea valley in an estuarine flow along the east side (left on the figure) of the sea valley. This higher salinity water is evident at Cape Kekurnoi (Reed and Bograd, 1995; Reed, 1987). The salinity gradients during spring were not as marked (Fig. 16). Without the large freshwater input, salinities were higher and more uniform across the shelf, but still the lowest salinities are found along the coast.

While thousands of conductivity-temperature and depth (CTD) casts have been made in the GOA, only two sites (separated by ~ 500 km) on the shelf have sufficient data to evaluate a seasonal signal. The longest record exists at GAK1 (the innermost station on the Seward Line) which has been maintained by the University of Alaska since 1970. The second site is at Cape Kekurnoi, the exit of Shelikof Strait, which has been maintained since 1984. Both stations are near shore and thus are impacted by the low salinity water of the ACC. The best data set is at the GAK1 site, because the time series is longer and the data are spread throughout the year. In contrast, measurements at Cape Kekurnoi were most often in the spring.

The seasonal signal of depth averaged temperatures and salinities at these two sites are similar

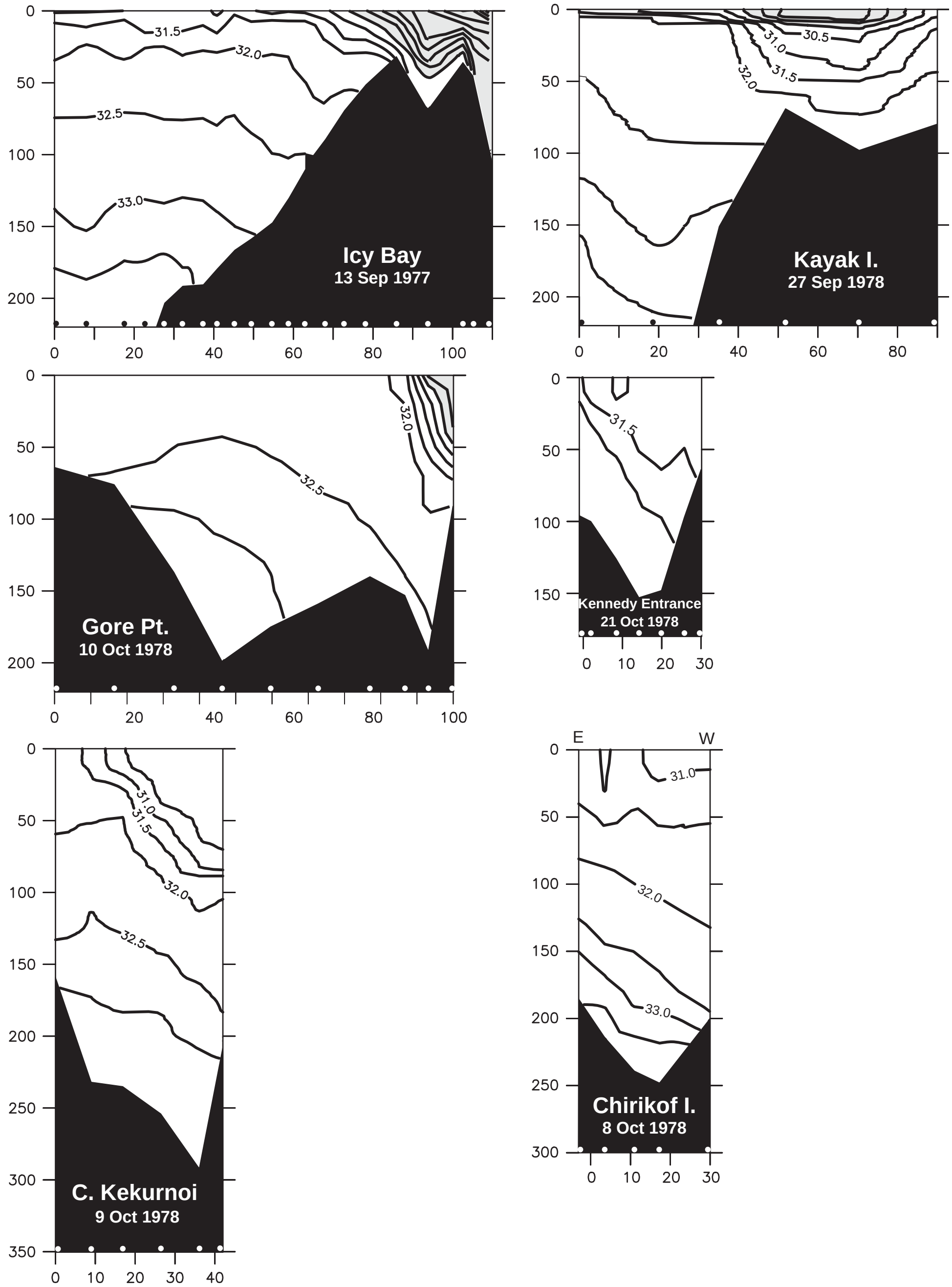

Fig. 15. Across shelf structure of the salinity (psu) during September and October at six sites along the shelf shown in Fig. 2. (1) Icy Bay, (2) Kayak Island, (3) Gore Point, (4) Kennedy-Stevenson Entrances, (5) Cape Kekurnoi at the exit of Shelikof Strait, and (6) line between Chirikof Island and Semidii Islands. The Alaska coast is to the right in panels 1–5. In panel 6 Chirikof Island is to the right. The shaded areas represent salinities <30 psu.

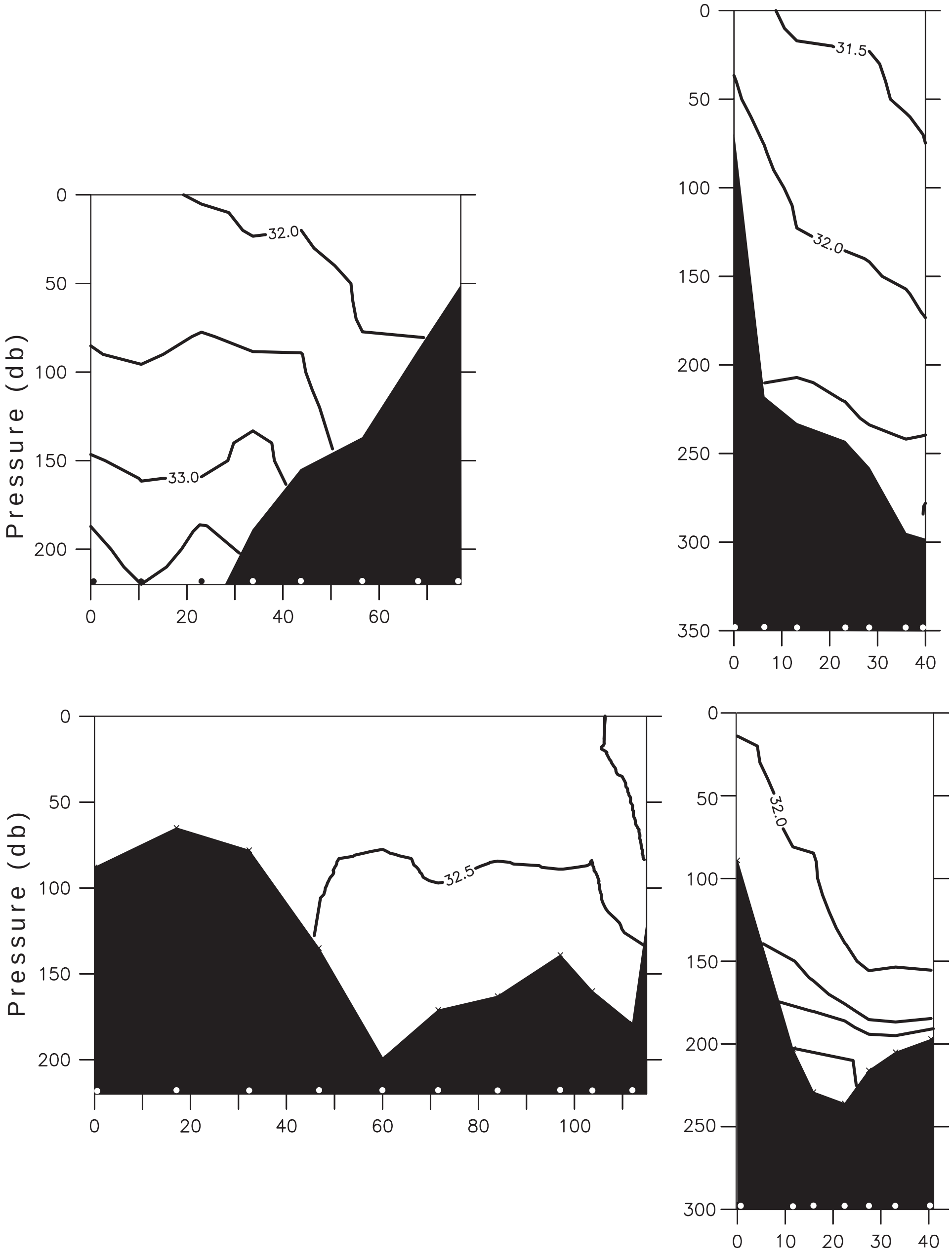

Fig. 16. Across shelf structure of salinity during May or early June at four sites along the shelf. (1) Kayak Island, (2) Gore Point, and (3) Cape Kekurnoi, (4) line between Chirikof Island and Semidii Islands. Once again the Alaskan coast is at the right of each panel.

(Fig. 17). At GAK1, there is a spread of almost 1 psu in the data and a distinct seasonal signal in the salinity, with the higher salinities occurring in late spring/early summer and lowest salinities in the fall. As expected, this is in phase with the time series of freshwater runoff, which also reaches a maximum in the fall. The seasonal temperature signal includes a broad minimum in March and a

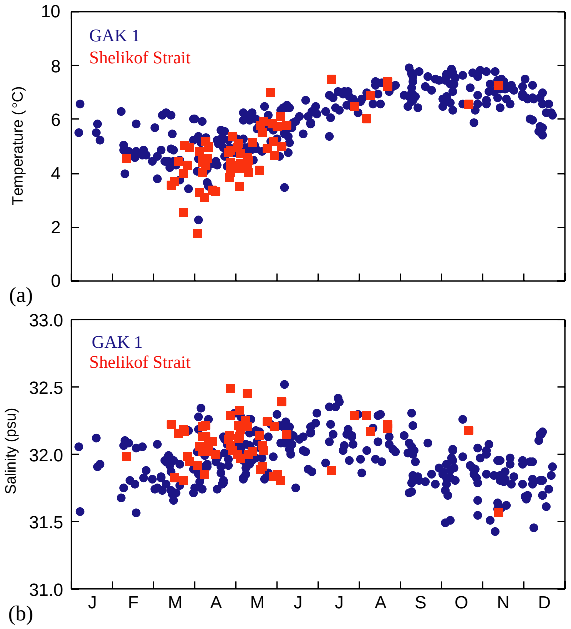

Fig. 17. Depth averaged (a) temperature and (b) salinity measured from CTD at GAK1 and Cape Kekurnoi. The blue circles indicate measurements at GAK1 and the red squares indicate measurements at a site near Cape Kekurnoi. Data are from 1976 to the present.

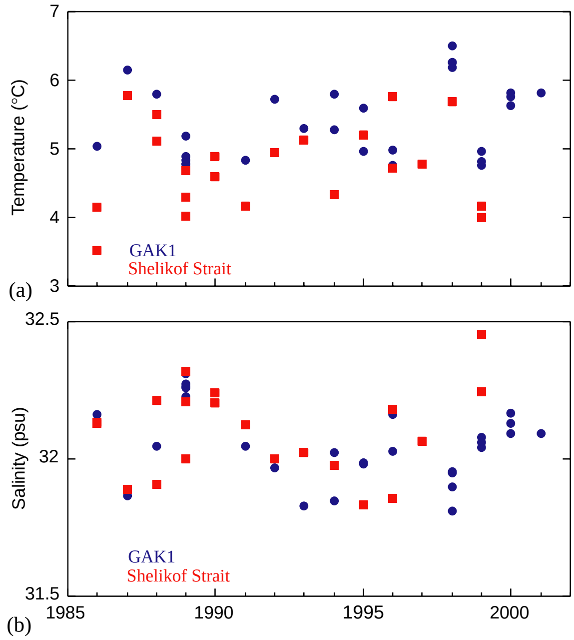

Fig. 18. Interannual time series of the depth integrated (a) temperature and (b) salinity at GAK1 and Cape Kekurnoi during May. All measurements were made using CTDs.

broad maximum in September. The lack of data collected during fall and early winter make it difficult to quantify a seasonal signal at Cape Kekurnoi, although trends in the sparse data appear similar to GAK1.

The best hydrographic data to examine the interannual variability on the GOA shelf are from May at GAK1 and Cape Kekurnoi (Fig. 18). Data exist for most years since 1985, with data at both sites for 12 of those years. The correlation between temperature at the two sites is $r = 0.80$ and between salinity is $r = 0.56$. As in the atmospheric time series, there is much year-to-year variability in the signals. The 1986–7 and the 1997–8 El Niños are characterized by warm, less saline water in 1987 and 1998, respectively. In contrast during the 1989 and 1999 La Niñas, the water column was cooler and more saline. This is expected, as El Niño events are associated with warmer winter-time air temperatures and greater precipitation, with the reverse true for La Niña periods. The shortness of the record precludes the ability to examine decadal variability, however, there was an increase in temperature and decrease in salinity at the outer end of the Seward line after 1977 (Overland et al., 1999b), which is generally recognized when there was well-defined regime shift in the North Pacific.

The annual cycle of near surface temperatures at GAK1 has a distinct seasonal signal with a maximum in August and minimum in March (Fig. 19, top). The cooling in the winter is largely due to the local surface heat fluxes. The lens of freshwater near the surface stabilizes the water column, permitting surface temperatures to often be colder than near-bottom temperatures. The annual temperature signal at depth is much weaker than that at the surface, with an indication of slightly warmer temperature in January. The data at Cape Kekurnoi (Fig. 19, bottom) are sparser and have been augmented with time series from current moorings (open circles and squares). The depth of the shallowest temperature sensor on most moorings was at 25–35 m, and thus well

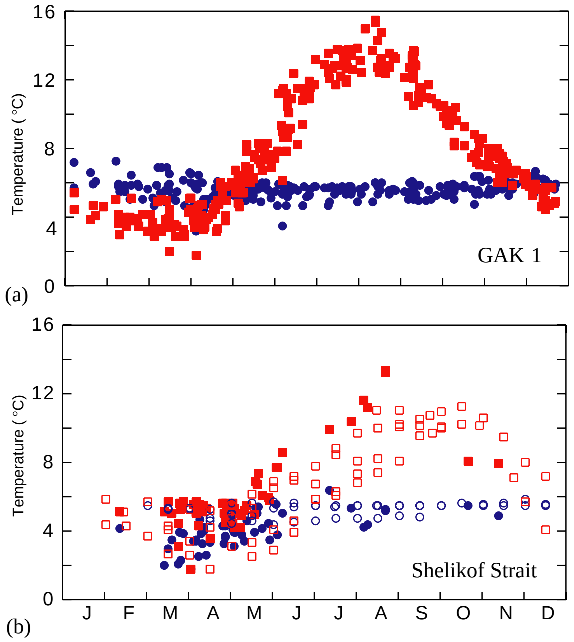

Fig. 19. Near surface (blue) and near bottom (red) temperature at (a) GAK1 and (b) Cape Kekurnoi. The open circles and squares are from current meter moorings, one point every 2 weeks. The bottom current meter was 10–15 m off the bottom and the top current meter was located 25–40 m from the surface.

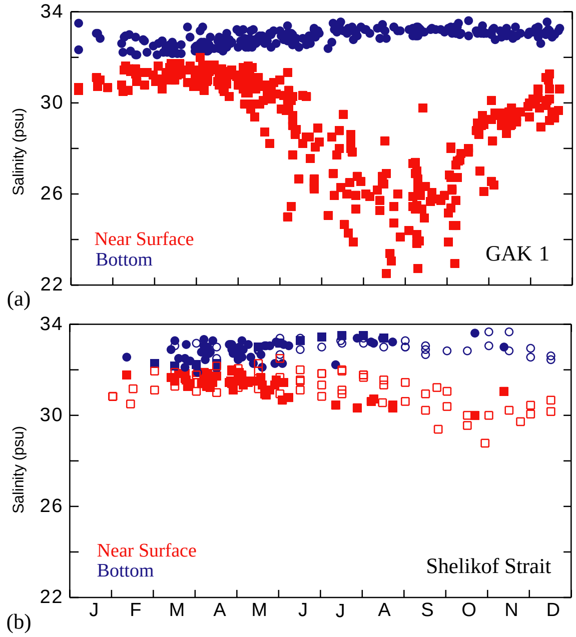

Fig. 20. Near surface (blue) and near bottom (red) salinity at (a) GAK1 and (b) Cape Kekurnoi. See Fig. 19.

below the surface. During winter this is not a problem since the surface mixed layer is typically greater than 35 m. During summer, however, the mixed layer can be shallower than 25 m. In general, the surface temperature signal at Cape Kekurnoi is similar to that at GAK1. The temperature at depth, however, is colder at Cape Kekurnoi than at GAK1 during February through April. This can be explained by mixing in Kennedy-Stevenson Entrances that results from the strong tidal currents there.

A strong seasonal signal in salinity exists at the Seward Line near the surface (Fig. 20a). As runoff increases and reaches its maximum in late summer and early fall (Fig. 3b), the ocean salinity at the surface decreases. During winter, runoff decreases and the surface salinity increases, while the vertical mixing and downwelling of the fresher surface water by strong winter storms reduces the salinity at depth. During summer, the salinity near the bottom increases once again, likely a result of an onshelf flux of slope water in response to relaxation of downwelling favorable winds. The seasonal cycle in near-surface salinity at Cape Kekurnoi (Fig. 20b) is much weaker than that at GAK1. In particular, near surface salinity during the summer is $\sim$3 psu greater than at GAK1 (the range in salinity from the current moorings is similar to that of the CTD casts). This supports the hypothesis that strong mixing occurs at Kennedy-Stevenson Entrance, where the fresher surface water is vertically mixed. Such an increase in surface salinity downstream of Kennedy Entrance was observed in 1978 (Fig. 3 in Schumacher and Reed, 1980). Vertical shear in Kennedy Entrance was calculated using data from a 150 kHz acoustic Doppler current profiler that was deployed in Kennedy Entrance in 1991 (Stabeno et al., 1995a, b). Bands of increased shear occur on fortnightly time scales, likely a result of tidal modulation (Fig. 21). The strongest vertical shears occurred at and above 100 m. This provides the energy necessary to mix the water column as the ACC flow through Kennedy Entrance and likely

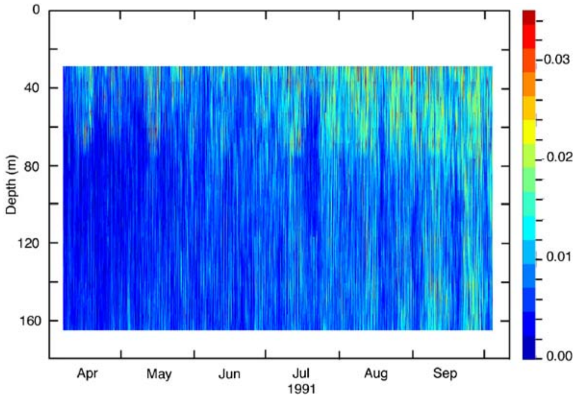

Fig. 21. Vertical shear (s^{-1}) at Kennedy Entrance as measured from 150 kHz ADCP. Bin depth was 4 m.

provides a pathway for the nutrients from the bottom of the water column to be exported into the euphotic zone.

3.4. Seasonal dynamics of nutrients and primary production

Seasonal variations of nutrients and production in the ACC are extreme. Aspects of seasonal primary production and nutrient distributions for the northern GOA have been reviewed, with focus mainly on the central Gulf and coastal regions (Sambrotto and Lorenzen, 1987) and in Shelikof Strait (Napp et al., 1996). There is little published data on the shelves east of Cook Inlet. Chlorophyll-*a* concentrations varied from $<1\,\mu g\,l^{-1}$ in winter to $>30\,\mu g\,l^{-1}$ during the spring bloom when surface nutrients are rapidly depleted (Napp et al., 1996). Annual C^{14} based production on the shelf is $\sim 300\,g\,C\,m^{-2}$ compared to $48\,g\,C\,m^{-2}$ at Ocean Station Papa (Sambrotto and Lorenzen, 1987).

In winter, cooling and storm winds weaken stratification, deepen the upper mixed layer, and entrain high concentrations of nutrients into surface waters. Deeper mixing of phytoplankton, a low solar angle, shorter photoperiod, and persistent cloud cover all limit irradiance to primary producers, and hence limit primary production in winter. In March–May, lengthening days, a higher solar angle and high nutrient concentrations lead to successional spring blooms of primary and secondary producers. There is significant interannual variability in the magnitude and timing of these blooms which are dependent on factors such as the extent of cloud cover, the intensity of stratification and grazing (Napp et al., 1996). Variability in the timing of spring production could disrupt predator/prey interactions and influence larval survival and recruitment (Napp et al., 1996; Freeland et al., 1997).

As phytoplankton growth is initially light-limited in spring, timing of the spring bloom over the entire shelf may be related to the extent of cloud cover (Napp et al., 1996; Townsend et al., 1994). Napp et al. (1996) examined the percentage of Total Opaque Sky Cover (%TOSC) in April above Kodiak, Alaska from 1952–1991. %TOSC is non-transparent cloud cover, which has the greatest attenuation on photosynthetically available radiation (PAR). For example, a 30% change in TOSC was related to a 25% change in mean daily PAR. The mean %TOSC above Kodiak in April varied from about 55–95%, with significant interannual variability in the mean %TOSC and in attenuation of PAR. Napp et al. (1996) argue that the spring bloom might be significantly delayed during years with the greatest cloud attenuation of PAR. While the extent of cloud cover might influence timing of spring production over large portions of the shelf, the influence of other factors such as riverine flow and stratification are more specific to the ACC.

Despite increased irradiance in early spring, stratification across the shelf remains weak. There is very little warming of surface waters from March through May (1–1.5° warming of surface waters relative to 150 m was observed in moorings along the Seward line, not shown), and freshwater discharge is near the seasonal minimum (Fig. 3b). The limited runoff generates weak salinity gradients in the ACC (Fig. 16, see also Reeburgh and Kipphut, 1987) causing the ACC to be slightly more stratified than other shelf waters. Napp et al. (1996) hypothesized that phytoplankton within the ACC are confined to a shallower mixed layer and exposed to greater solar irradiation than other plankton on the shelf, and therefore might be expected to bloom earlier. Yet such generalities are difficult to apply in early spring due to significant mesoscale spatial variability and small gradients in physical parameters on the shelf. For example, in 1998, relatively high fluorescence was observed not only in the ACC, but also in surface waters at the shelf break (Fig. 9).

Nitrate data are too sparse to examine the hypothesis that the shelf bloom initiates in the ACC. Surface maps of nitrate data in the ACC show relatively high concentrations in early spring and depleted concentrations in mid-to-late summer (Fig. 22), but adequate spring and summer hydrographic sections across the ACC are not yet available to address this question.

In late spring and early summer (May–June) intense chlorophyll blooms and low surface nutrients are observed across the shelf. Composites of satellite ocean color from May 1997, 1998, and 1999 show intense and patchy blooms throughout the coastal GOA (Fig. 9). The satellite images reveal a sharp contrast between the highly productive, iron-rich and spatially variable waters of the shelf compared to the moderate and more uniform production of the iron limited central GOA (Martin et al., 1989). Exchange between coastal waters rich in chlorophyll with central GOA waters rich in macro-nutrients during 1997–1999 is evident in the form of swirls, eddies, and filaments of high chlorophyll extending into the central GOA and regions of low chlorophyll impinging on the coast.

Sections of nitrate at Gore Point and at the Seward line in May 2001 show low surface concentrations with strong vertical structure (Fig. 23). At Gore Point, the highest nitrate concentrations in the surface waters were along the coast. At Seward, concentrations in the surface waters near the coast were very low ($<2\,\mu$M), while at each of the other stations concentrations were typically above $10\,\mu$M. The highest concentrations were at the slope below 100 m, with intrusions of the nitrate rich water evident on shelf below $\sim$120 m.

In summer there is strong stratification across the shelf. These months of increasing riverine discharge result in the fresher waters of the ACC

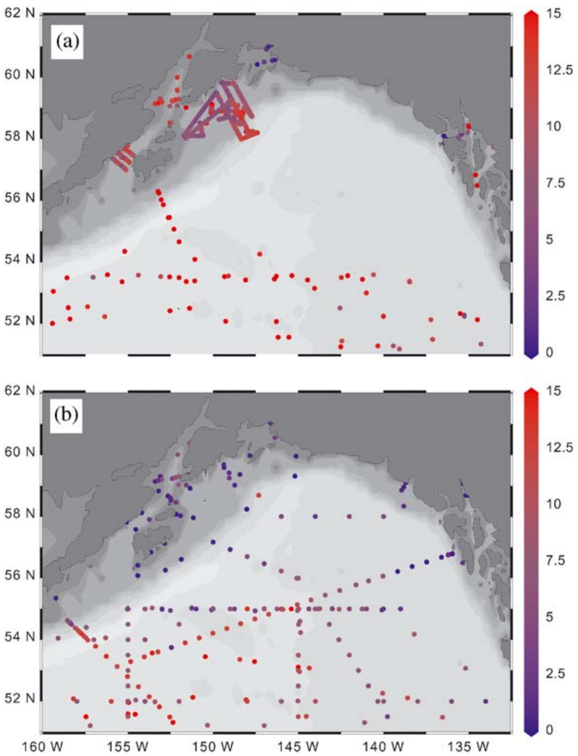

Fig. 22. Surface nitrate maps. (a) March–May, (b) June–September. These are data from NODC, several FOCI cruises and a GLOBEC cruise in May 2001.

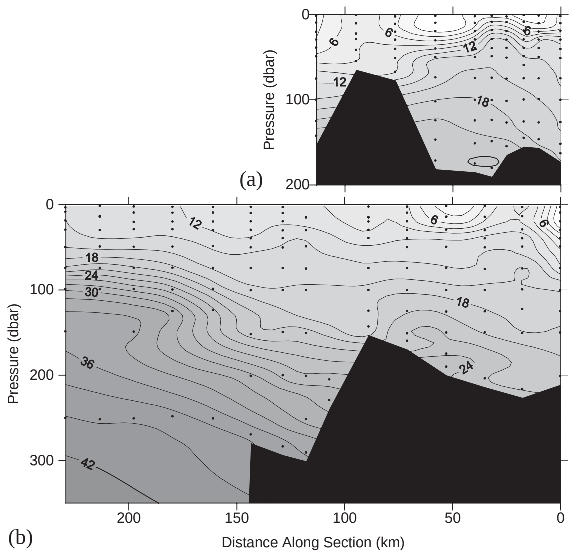

Fig. 23. Concentrations of nitrate at two locations along the Kenai Peninsula, (a) Gore Point and (b) Seward line. Data was collected in May 2001. Dots indicate location of data points. The coast is at the right in each plot.

confined near the coast, and an intense thermocline at $\sim$25 m extending over the remaining shelf. In these stratified surface waters, nutrients are depleted, with concentrations increasing below the pycnocline (not shown). Measurements of iron over the shelf are sparse. However, what data exists support the hypothesis that iron and nitrate have similar distribution over the shelf in summer. Concentrations are depleted at the surface, and increase below the pycnocline (Martin et al., 1989), except in fresher waters of the ACC, where riverine discharge may supply ample iron.

A sub-surface chlorophyll-*a* maximum is often associated with a strongly stratified surface layer depleted in nutrients. Pigment concentrations are highest at the base of the euphotic zone where nutrients are supplied from the pool nutrients below the pycnocline through diffusion, diapycnal and tidal mixing (Whitney et al., 1998; Sharples et al., 2001). Along the Seward Line, such an intense sub-surface fluorescence maximum was observed above thermocline. The seasonal distribution of nutrients and chlorophyll-*a* near the Seward Line evolved from spring conditions (a fluorescence maximum in the ACC and strong horizontal gradients) to mid summer conditions (depleted nutrients at the surface, a subsurface chlorophyll-*a* maximum independent of the ACC, and intense vertical gradients associated with the pycnocline).

To examine the spatial patterns of surface chlorophyll-*a* during summer, a composite chlorophyll-*a* image was created using SeaWifs L1A data. We averaged non-cloudy pixels from summer (June 15–August 30) images collected in 1998–2002. Pixels at high zenith angles ($>60^\circ$) or within two pixels of land or clouds were excluded. We did not exclude pixels where turbidity was high. The SeaDas level-2 processing flagged turbidity in the near coastal (i.e., orange area east of Prince William Sound) and in Cook Inlet, but rarely elsewhere. High turbidity can either mask or enhance chlorophyll.

There is a marked difference between chlorophyll-*a* concentrations east of the Gore Point line (Fig. 2) and west of it. Summer surface chlorophyll production in the GOA was concentrated along the shallower banks south of Kodiak Island, the region northwest of Kodiak Island, and in Shelikof Strait. Concentrations along the Kenai Peninsula are markedly less than those observed farther west, indicating there was not a persistent infusion of nutrients into the surface mixed layer during summer. The higher concentrations of chlorophyll in Shelikof Strait support the conclusion that mixing in Kennedy Entrance supplies nutrients into the euphotic zone. A large portion ($\sim$25–50 km wide) of the shelf east and south of Kodiak Island is shallow ($<$50 m) and may be susceptible to significant tidal mixing. The extent of stratification and surface nutrient depletion across this shallow shelf in summer are uncertain. Drifter tracks do show a highly convoluted flow with sufficient energy to widely distribute any surface waters enriched in nutrients and chlorophyll-*a*.

In lower Cook Inlet, high nitrate concentrations are observed all summer (Larrance and Chester, 1979; Sambrotto and Lorenzen, 1987). In mid-to-late summer, concentrations of 5–10 μM are observed in southeastern Cook Inlet in contrast to undetectable to 2 μM concentrations along the shelf to the east (Fig. 22). Drifter studies indicated that the ACC enters Cook Inlet to the east, and undergoes only a slight excursion northward. Mixing that occurs in Kennedy Entrance may contribute to the nutrient supply at the exit of Cook Inlet. Certainly, high concentrations ($>$14 μM) of nitrate existed at a depth of 50 m at both the Seward line and at Gore Point (Fig. 23) in May 2001. Measurements of vertical shear at Kennedy Entrance (Fig. 21) indicated mixing to greater than 50 m. These observations suggest that tidally driven (persistent) deep mixing in Kennedy Entrance and likely in southeast Cook Inlet continually supplies nutrients to the surface. This steady nutrient supply to surface waters sustains high production rates even in mid-to-late summer (Larrance et al., 1977) making lower Cook Inlet one of the most productive high-latitude shelf regions in the world (Sambrotto and Lorenzen, 1987).

Transport of surface pigments and nutrients by the ACC from Cook Inlet through Shelikof Strait might contribute to the high chlorophyll-*a* concentrations observed in the northern strait (Fig. 24);

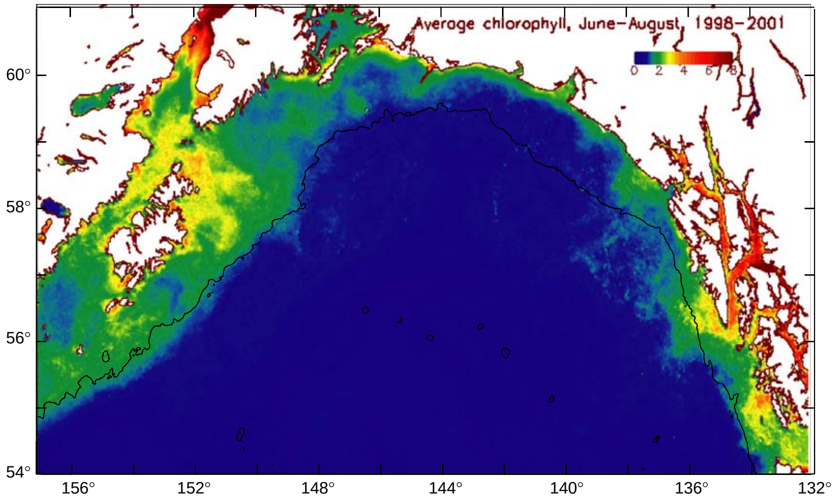

Fig. 24. The average concentrations of chlorophyll-*a* during June 15–August 30 (1998–2002) as measured from SeaWiFs. The method of averaging is described in the text. The 100 m and 1000 m isobaths are shown. The high concentrations of chlorophyll-*a* along the coast (<100 m) from Icy Point to Prince William Sound may not be reliable due to high turbidity.

however, off Cape Kekurnoi, nitrate depletion has been observed as early as May on the peninsula (northern) side of the sea valley (Napp et al., 1996). Resident times of phytoplankton from Cape Douglas (58°16′, 153°16′) to Cape Kekurnoi are estimated at 7–18 days; given production estimates of 100–300 $g\,C\,m^2\,yr^{-1}$ over 180 d and 50 m of water, this equals the consumption of 1–8 μM nitrate within Shelikof Strait, values similar to the observed concentrations in lower Cook Inlet. This calculation suggests that additional nutrient introduced through vertical mixing support high pigment concentrations during summer observed in southern Shelikof Strait (Fig. 24).

Another possible source of nutrients is the estuarine inflow in the Shelikof sea valley. There is significant interannual variability of ACC transport through Shelikof Strait. Years with strong ACC flow can induce an estuarine-like deep return flow up the sea valley. This return flow is concentrated on the Kodiak Island side (southern) of the sea valley (Napp et al., 1996) and is thought to entrain nutrients into the upper layer due to intense horizontal sheer and turbulence. Hence, the southern extent of high chlorophyll-*a* in Shelikof Strait appears to be a function of the continuity of flow through the strait, the supply of nutrients upstream, and phytoplankton grazing.

4. Mechanisms for cross-shelf fluxes

Major questions remain on how nutrients and zooplankton are advected onto the shelf in this highly productive, predominantly downwelling regime. Several mechanisms exist which result in cross-shelf fluxes of nutrient rich waters from the deep basin, although many are transient in nature and thus difficult to detect. We next examine some likely mechanisms supported (or refuted) by the data.

4.1. Episodic upwelling

Even though this is predominantly a downwelling regime, during summer winds relax and periods of upwelling occur, which result in increased salinity at depth, as observed at Seward Line (Fig. 20). As there is a significant correlation between salinity and nutrients (Mordy et al., submitted), increased salinity during the summer months at the bottom of the water column implies a source of nutrient rich water. However, our analysis of wind data suggests that upwelling events are rare to the east of the Shumagin Islands. Hence this mechanism is unlikely to provide a consistent source of nutrients in the observed areas of high production. During the summer, the relaxation of the strong downwelling winds and the resulting depression of the pycnocline can result in increased salinity and nutrients near the bottom.

4.2. Surface flux in the Ekman layer

The central GOA is characterized as a high nutrient-low chlorophyll (HNLC) region. Upwelling in the central gyre supplies an abundance of macro-nutrients to the surface through winter entrainment across a deep and weakly stratified mixed layer (Whitney et al., 1998). In summer, chlorophyll-*a* concentrations remain relatively low despite abundant nutrients, warmer temperatures, stronger stratification, and increased irradiance. This is presumed due to a combination of factors: (1) the predominance of small zooplankton which continually graze phytoplankton and hence prevent large blooms from depleting the nitrate (Frost, 1991); (2) the absence of sufficient iron to support such blooms (Martin and Gordon, 1988; Martin et al., 1989). Whatever the cause, the observed high values of nutrients could provide a significant source of nitrate to the coastal areas through simple Ekman flux, driven by the downwelling favorable winds. The high productivity of the CGOA may be fundamentally due to the convergence of the offshore waters, rich in nitrate, with the coastal waters, rich in iron. Indeed, some SeaWiFs chlorophyll imagery suggests highest productivity at the interface between the coastal and offshore waters.

Numerical simulations of circulation can be used to help infer patterns of onshelf transport in the CGOA. To investigate cross-shelf transport, we have seeded numerical floats in a regional model of the area (Hermann et al., 2002). Floats were uniformly seeded over areas with bathymetry in the range of 1000–3000 m (Fig. 25a). These were tracked, at two different fixed depths (5 and 40 m), using a 2-month series of model hindcast daily mean horizontal velocities for late fall 1996. Many of the floats tracked at the shallow depth move vigorously across isobaths, from the slope onto the shelf (Fig. 25b). Preferred sites for onshore movement include areas to the east and south of Prince William Sound, whereas onshore flux is weak across the Alaska Stream and in the vicinity of the Sitka eddy. This broad pattern of cross-shelf transport is consistent with the spatial pattern of observed climatological surface nitrate (Conkright et al., 1998), which exhibits a tongue of high nitrate waters penetrating onto the shelf to the southeast of Prince William Sound. Floats tracked at a deeper (40 m) depth (not shown) exhibit substantially weaker onshelf flux; instead, they followed the isobaths, with none entering onto the shelf. The time-averaged wind stress used for these simulations is typical of the fall season. This result supports that an Ekman flux from the basin can be a source of nutrients.

A simple calculation indicates that sufficient nutrients can be supplied via this mechanism to account for the observed primary production. Estimates of downwelling and runoff-driven production on the shelf may be made as follows: assume that 100–300 $g\,C\,m^{-2}$ (8.3–25 $mol\,C\,m^{-2}$) of new production is generated each year on the shelf. Given a standard Redfield ratio for the elemental composition of new production

$$C : N : P : Fe = 106 : 16 : 1 : 0.01,$$

annual nitrogen and iron requirements would be 1.3–3.8 $mol\,N\,m^{-2}$ and $7.8–24 \times 10^{-4}\,mol\,Fe\,m^{-2}$. For a productive area of 50–250 km wide, a km of coastline would require $6–94 \times 10^{7}\,mol\,N\,yr^{-1}$ and $4–59 \times 10^{4}\,mol\,Fe\,yr^{-1}$.

Nitrate concentrations in the upper 100 m over the deep basin of the GOA range from 10 to 20 $\mu mol\,l^{-1}$, or 0.01 to 0.02 $mol\,N\,m^{-3}$. A surface layer 40 m thick moving towards the coast at 0.025 $m\,s^{-1}$ would supply roughly $16–32 \times 10^{7}\,mol\,N$ along each km of coastline during 6 months of strong downwelling conditions. This represents sufficient nitrogen for highly productive narrow shelves, but insufficient to sustain the highest production over wide shelves. (The chosen value of 0.025 $m\,s^{-1}$ over 40 m is in fact sensible; for a typical wind stress of 0.1 $N\,m^{-2}$ and a Coriolis force of $\sim 1.0 \times 10^{-4}\,s^{-1}$ at 45°N, the total Ekman flux, is 1000 $kg\,m^{-1}\,s^{-1}$, or 1 $m^{3}\,m^{-1}\,s^{-1}$.)

Royer's discharge values suggest an average discharge of $2 \times 10^{4}\,m^{3}\,s^{-1}$ along the length of the CGOA coastline in spring and early summer. If these waters contain 3 $\mu mol\,l^{-1}$ of Fe, then

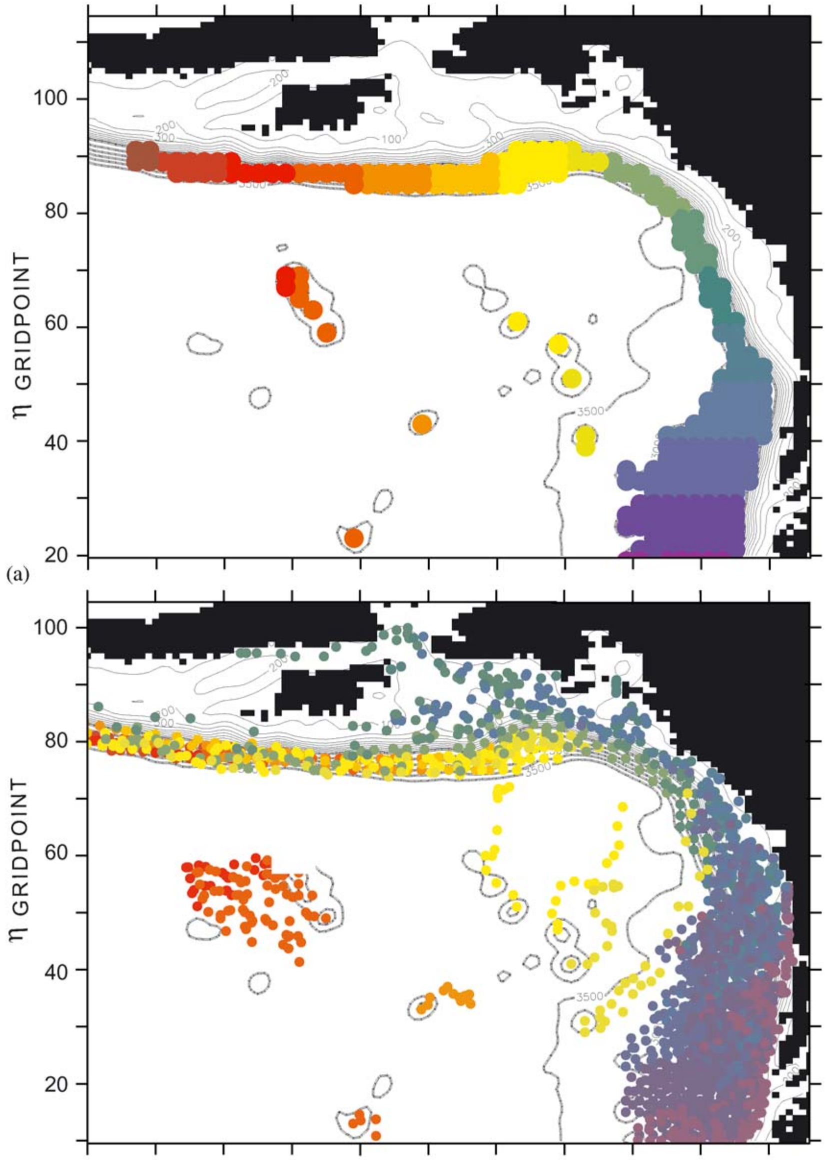

Fig. 25. Locations of floats (a) seeded into model velocity field at a depth of 5 m and (b) position of the floats after 50 days.

60 mol Fe s^{-1} would be added to the shelf, i.e., 19×10^8 mol Fe yr^{-1}. If the runoff is assumed distributed over a 1000 km section of coastline, this corresponds to 190×10^4 mol Fe yr^{-1}, in excess of the required value. This is not the only possible source of Fe. Winds blowing off land may deposit Fe over the shelf. In addition, strong currents may resuspend sediments and perhaps be a source of Fe to the euphotic zone. There is insufficient data to identify which of these are the most important sources.

Obviously, the above argument uses very crude estimates. However, it suggests that even as much as 200–300 g C m^{-2} yr^{-1} production could be supported on the shelf, through the combination of downwelling-supplied surface nitrate from the deep basin and runoff-supplied iron at the coast. However, near-surface nutrient concentrations in the central GOA are highly variable, and may be decreasing (Freeland et al., 1997). So while this mechanism may replenish nutrients to the shelf during winter and early spring, it is not a reliable source during summer.

4.3. Upwelling seaward of a coastal wind jet

The steep and prominent terrain surrounding the GOA causes systematic spatial patterns in the winds, which can produce important variations in the surface Ekman transports discussed in the previous section. In particular, the coastal terrain of the GOA forces a phenomena known as a barrier jet (Parish, 1982), in which enhanced along-shore winds occur in the nearshore region relative to farther offshore. In conditions of cyclonic atmospheric flow over the GOA, the cross-shelf gradients in the winds can result in substantial, positive wind stress curl, and hence local upwelling off the coast, but typically inshore of the shelf break (Fig. 26).

Barrier jets tend to occur when the cross-shore component of the large-scale low-level flow is directed onshore, the along-shore component is with the terrain on the right (in the Northern Hemisphere), and the static stability from the surface to mountain crest level is moderate (Overland and Bond, 1995). Barrier jets are expected to occur in the eastern and northern GOA during southerly and southeasterly flow, respectively, which is a common occurrence during fall through spring. The potential enhancement of wind speeds associated with barrier jets scales linearly with the height of the coastal terrain (Overland and Bond, 1995); this mechanism therefore includes significant along-coast variations in magnitude. The barrier jet extends approximately one Rossby radius offshore ($\sim$50–100 km for the GOA). The positive wind stress curl at this location tends to be concentrated over a narrow ($<$20 km) band due to frontogenetical stretching within the atmospheric boundary layer.

We do not know the full implications of a barrier jet for the mixed layer over the shelf of the northern GOA, but rough estimates of its frequency and magnitude suggest that it could be

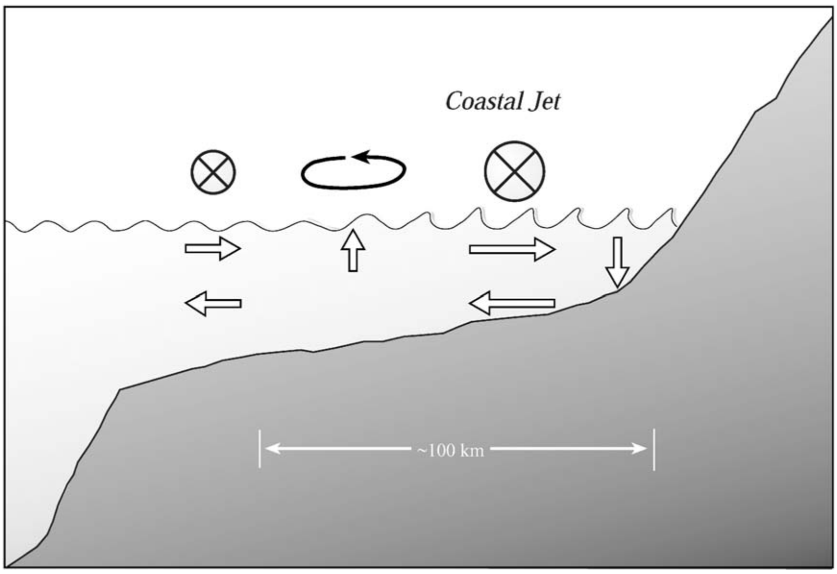

Fig. 26. Schematic of the coastal wind jet and its effects on the upper mixed layer. The circled X's indicate the strength of the winds into the plane of the figure; the cross-shore gradient in these winds produces a region of strong positive wind stress curl. The open arrows indicate the cross-shore component of the wind-driven ocean circulation in these conditions.

important. Conditions favorable for the development of barrier jets appear to occur approximately one-third of the time during the cool season, based on our perusal of SAR-derived winds during 1999–2000. Following Overland and Bond (1995) and Doyle and Bond (2001) and based on our experience in analysis of the weather of the region, we assume that barrier jets typically result in near-shore wind speeds of 14 m/s, off-shore speeds of 10 m/s, and that the cross-shore gradient of the resulting wind stress is distributed over a width of 20 km. These values, combined with a frequency of occurrence of one-third, yields an average Ekman pumping velocity of approximately 10 m per day. This vertical velocity is comparable to that found by Munchow (2000) for the region off Pt. Conception, California, where topographical effects cause similar spatial gradients in the winds. Its magnitude suggests that local upwelling over the shelf, in conditions of downwelling favorable winds in the immediate vicinity of the coast, could play an important role in nutrient supply to the shelf in the GOA, especially during late fall through spring. During summer the winds are weaker, and this mechanism probably is not a significant source of nutrients to the shelf.

4.4. Topographic steering

Coastal flows are strongly steered by bathymetry, and the region from Icy Bay to the Shumagin Islands is rich in large bathymetric features such as Hinchenbrook Canyon, Amatouli Trough and the Shelikof sea valley, in addition to many smaller troughs. Given the right circumstances, topographic features interact with currents in many ways that result in on shelf fluxes of slope water (Allen et al., 2001). For instance, the ACC flows parallel to the axis of the Shelikof sea valley, which results in an estuarine-like inflow (Reed et al., 1987; Stabeno and Hermann, 1996). This intrusion of slope water extends past Cape Kekurnoi and is entrained in the strong ACC, providing nutrients to surface waters. Neither Hinchenbrook Canyon nor Amatouli Trough, however, appear to have estuarine flow, although onshelf flux is evident in the model result at Amatouli Trough (Fig. 11). An examination of mean flow at a number of mooring sites located in canyons or troughs reveal a consistent pattern. There is flow into the trough on the east side and outflow on the west side in the bottom 50 m (Fig. 27).

Klinck (1988) proposed that inertial overshoot of an along-shore flow intruding into a canyon could lead to significant onshelf flux of deeper waters. However, he demonstrated how such onshelf transport is stronger when the shallow bathymetry is to the left of the direction of the along-shore flow in the Northern Hemisphere, and much weaker when the bathymetry is to the right of the flow. In the GOA, the coast is typically to the right, hence the inertial overshoot mechanism is less important.

A third mechanism describes the interaction of downwelling and canyons. In a downwelling regime, water accumulates at the surface within a Rossby radius of the coastline and the subsurface pycnocline and nutricline are depressed. The surface pressure gradient acts in the offshore direction, whereas (for a two-layer flow at least) the subsurface pressure gradient acts in the onshore direction. Along a straight coastline, these pressure gradients are mainly balanced by the Coriolis force. Narrow canyons, which cut across an otherwise straight shelf, have weak flows at

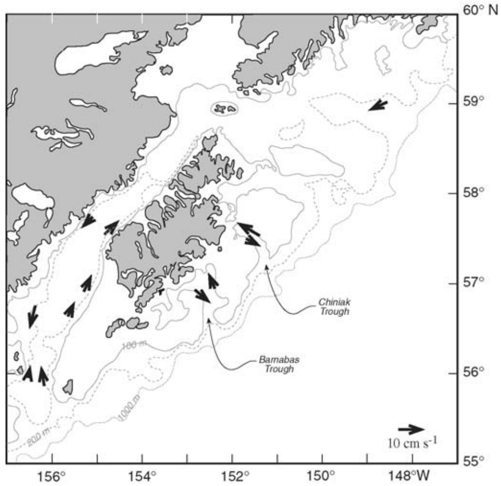

Fig. 27. Since 1984 a number of moorings have been deployed in troughs and canyons along the GOA coast. The bold arrows represent the mean flow at ~15 m off the bottom.

depth and so any cross-shelf pressure gradients may push the deeper, nutrient-rich waters onto the shelf. We cannot presently quantify the magnitude of this source to the shallow GOA, but further model studies at fine (~ 1 km) resolution can be used to address this issue.

The interplay of canyons and shallow banks can provide a steady although localized supply of nutrients to the euphotic zone over the shelf. Nutrient rich slope waters transported up canyons can upwell onto banks. Strong tidal mixing on the banks can introduce nutrients into the upper water column. The complexity of bathymetry in the GOA, and the higher primary production at the surface in the vicinity of Kodiak Island (Fig. 24) support this as a possible mechanism for the introduction of nutrients onto the shelf and eventually into the euphotic zone not only during winter but throughout the year.

4.5. Eddies

Large (~ 200 km) eddy features, most dramatically illustrated by AVHRR imagery reported in Thompson and Gower (1998), may play a significant role in cross-shelf exchange. When these large eddies impinge on the slope in the northern CGOA, they may advect deep, nitrate-rich waters onto the shelf. Model results suggest a significant flux of waters off the shelf in the vicinity of the large, semi-permanent eddy near Sitka, Alaska (Hermann et al., 2002). This cross-shelf exchange may serve to mix the iron rich, nitrate poor shelf waters (summer) with the nitrate rich, iron poor basin surface waters. It has been suggested (Paul Harrison, personal communication) that eddies containing iron-rich shelf water might account for observed periods of higher productivity at Ocean Station P.

An example of interaction of an eddy with shelf occurred in 2001 (Fig. 28). A large eddy was evident in the basin seaward of Prince William Sound in May. It slowly migrated along the slope and eventually, in late July, could be found off the Kenai Peninsula, where it remained largely stationary for approximately a month, with a second weaker eddy persisting slightly to the northeast. A number of satellite tracked drifters were deployed in May and July between Kayak Island and Gore Point. Trajectories of three of the drifters show the complexity of flow that resulted from the close proximity of the eddy. One drifter (dark blue) was drawn off the shelf between the two eddies, while another drifter (light blue) left the shelf near Kayak Island. A third drifter (black) was drawn off the shelf, moved eastward along the slope and returned to the shelf near Hinchinbrook Canyon. Other drifters further on the shelf, show no response to the eddy. Eddies, like topographic steering, can increase on/off shelf exchange year round, but the impact is localized to outer portions of the shelf. In contrast, the on shelf flow due to Ekman fluxes impacts broad areas, but the primary effect is during the cold season. The productivity of the shelf is likely dependent not on a single mechanism, but rather on a variety of sources.

5. Discussion

Our purpose in this section is to summarize knowledge and gaps in our understanding of the coastal meteorology and oceanography of the GOA, especially as it pertains to the forcing of the ACC. We first discuss the nature of the temporal variability on scales from decadal to sub-seasonal, and then outline issues related to the downscaling of the large-scale atmospheric circulation to the coastal conditions. Finally, we discuss the effects of physical forcing on the nutrient supply of the shelf.

The 50-year record of GOA coastal weather permits consideration of decadal scale variations. With regard to winter, it is instructive to compare our time series with the leading mode of variability for the North Pacific as a whole, the PDO. As evident in Figs. 6 and 8, the relationship between the PDO and GOA coastal weather is actually quite weak. There are tendencies for relatively warm winters in the northern GOA, and anomalous southerly winds in the eastern GOA, during positive phases of the PDO (and vice versa), but for the most part, the fraction of the variability that occurs on decadal time scales is much greater for the PDO than for the coastal weather of the

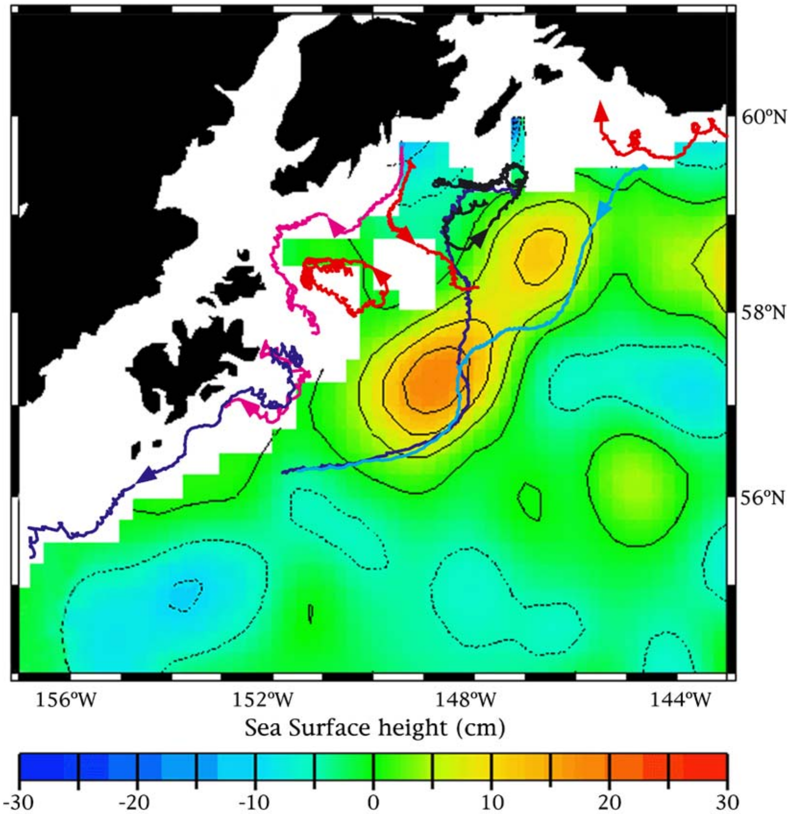

Fig. 28. Trajectories of satellite tracked drifters (drogue depth 40 m) overlayed on TOPEX and ERS-2 altimeter data based on 10 days of TOPEX (August 4–14, 2001) and 17 days of ERS-2 (July 27–August 14, 2001). Maps were provided courtesy of Colorado Center for Astrodynamics Research on their Global Near Real-Time Sea Surface Height Data Viewer web page. The drifter trajectories are approximately 1 month long.

GOA. The lack of a significant PDO signature in the coastal GOA can be attributed to three factors: (1) the PDO itself accounts for only about a third of the variance in SST during winter over the North Pacific (Hare, 1996; Overland et al., 1999a, b), (2) the PDO largely reflects the state of the atmosphere–ocean climate system in the west-central North Pacific and the GOA is only weakly out of phase with this region, and (3) the large-scale pressure anomalies driving the weather of the coastal GOA are poorly correlated with the SST anomalies. While the coastal weather of the GOA does not appear to be tightly coupled to the PDO, the wind forcing of the central portion of the basin might be. At least the 1977 regime shift of the PDO seems to be well represented in the sequence of central GOA dynamic height anomalies documented by Lagerloef (1995). We consider it an open question whether decadal variability in the deep basin of the GOA, presumably through its modulation of the Alaskan Stream, influences the ACC. The lack of long-term oceanographic data, however, makes it difficult to resolve the relationship. A better understanding of the linkages between the atmosphere and ocean, and between the basin and the shelf is being pursued through the observational and modeling work for the northern GOA undertaken as part of GLOBEC.

We also examined a 50-year record of summertime conditions in the coastal GOA, and the decadal variability for this time of year is also relatively weak. We had expected to find systematic summertime weather anomalies in the 1990s different from those in the 1980s, because the two leading modes of spring/summer climate variability for the North Pacific were of opposite sign in the two periods (Overland et al., 2001). The results found here (Figs. 5 and 7) suggest that the coastal weather of the GOA is more sensitive to local rather than to basin-scale atmospheric circulation anomalies.

Part of the variability of the coastal GOA on 2–7 year time scales is linked to ENSO. Here, the principal impacts are on wintertime precipitation, and hence runoff, including the timing of runoff, since precipitation and air temperature are positively correlated in coastal GOA watersheds (e.g., Bitz and Battisti, 1999). The coastal winds do not seem to be sensitive to ENSO, and so changes in sea level in the ACC in association with ENSO may be caused more by coastally trapped Kelvin waves emanating from the tropical Pacific (Enfield and Allen, 1980; Chelton and Davis, 1982) than by anomalous local forcing. In spring, there was a response to ENSO in the salinity and temperature at GAK1 and Cape Kekurnoi, which is likely a combination of propagation of coastal signal and response to local forcing. Changes in transport of the ACC are not expected because the coastal winds are not very sensitive to ENSO.

Since the atmospheric basic state is much different in the summer than in the winter, the atmospheric response in the eastern North Pacific to ENSO is different for the two times of year. In particular, Overland et al. (2001) showed that anomalously high pressures occur over the GOA during El Niños in the summertime, while anomalously low pressures are found in the wintertime. Based on our examination of coastal weather records, we conclude that this difference is manifested more in the central GOA than in its coastal margins.

We have concentrated on the interannual fluctuations in coastal GOA weather in this paper, but for completeness, we now briefly discuss its sub-seasonal variability. The weekly to monthly variability during the winter serves to modulate the frequency, intensity, and nature of the individual storms that determine the transport of ACC. The preponderance of one or the other of the two most important sub-seasonal weather regimes, that is high-amplitude ridges or troughs at geopotential heights at 500 hPa over the North Pacific, is linked to large-scale, long-term circulation anomalies associated with the PDO and PNA (e.g., Renwick and Wallace, 1996). The summertime sub-seasonal variability has received less attention, but from our experience, the GOA is marked by swings between cyclonic regimes, which feature more downwelling favorable coastal winds and enhanced coastal rainfall, and anticyclonic regimes, with weakly upwelling favorable winds and suppressed rainfall. The timing of the transitions between these summer weather regimes is important to the ACC and its marine ecosystem. Periods of weak winds result in a lack of transport down Shelikof Strait. This decrease results in a decrease in the estuarine flow up the Shelikof sea valley and a reduction in nutrients available to the west of Kodiak Island. In addition, a lack of organizing winds result in a more convoluted flow along the Kenai Peninsula which also may impact the replenishment of nutrients to this part of the shelf, although whether to decrease or increase it is not known. Certainly, reduced transport through Kennedy Entrance will both reduce the nutrients that are mixed in Kennedy Entrance and their advection down stream in Shelikof Strait. Noting this, we suspect that short-term events, such as the occasional strong storm or periods of upwelling, are relatively more important to the ACC in the summer than in the winter, when winds are stronger. There is some evidence that the incidence of such events has a weak relation to the slow manifold of climate variability (Minobe and Mantua, 1999).

In summary, we find most of the variability in atmospheric forcing and ocean response to be on seasonal or shorter time scales. In terms of the coastal meteorology and oceanography decadal signals are relatively weak. However, while it appears that much of the GOA ecology is adapted to this seasonal variability, the biology appears to be responsive to the weak decadal signals (Hare and Mantua, 2000). The pathways that determine this connection are not known, but some relationships have been hypothesized (Gargett, 1997; Francis and Hare, 1994).

Decreased winter convection and nutrient entrainment in the central gyre are predicted to be a consequence of long-term global warming (Woods and Barkmann, 1993). Indeed, over the past several decades, central GOA surface waters have warmed and freshened. Long-term records of SST and salinities at Ocean Station Papa (OSP) and at coastal stations in British Columbia reveal a 0.4–1.0 century^{-1} decrease in salinity and a 1–2°C century^{-1} increase in temperature (Freeland et al., 1997; Whitney et al., 1999). As predicted, this region has experienced increased stratification, thinning of the mixed layer, and reduced winter entrainment of nutrients (Freeland et al., 1997). Along Line-P, south of the GOA, the extent of seasonal nutrient depletion was more widespread in the 1990s relative to historic (1970s) observations (Whitney et al., 1998). It has been estimated that associated with lower nitrate concentrations along Line-P, chlorophyll concentrations are about half of historic levels (Whitney et al., 1999).

The 1997–98 ENSO event had a similar impact to that predicted for secular warming on the nitrate and chlorophyll-*a* fields. With both PDO and ENSO in the warm phase, extremely large SST anomalies (>3°C) were observed all along the west coast of North America. Warmer waters increased buoyancy of the winter mixed layer, suppressing winter entrainment and coastal upwelling Along Line-P, nutrient concentrations were about half as large as observed in the 1970s with nutrient depletion occurring 1 month earlier than in previous years (Whitney et al., 1999). In May, 1998, chlorophyll-*a* concentrations were low over the entire GOA shelf, presumably from a reduced supply of nutrients (Fig. 9; Whitney and Welch, 2002).

One approach to better understand the extent of upwelling in the central GOA and coastal downwelling is through analysis of pCO$_2$, which is a sensitive measure of vertical fluxes. A number of papers have examined the North Pacific CO$_2$ based on large-scale survey cruises (e.g., Landrum et al., 1996; Murphy et al., 1998), ship-of-opportunity data between the US and Asia (e.g., Takahashi et al., 1993; Stephens et al., 1995; Murphy et al., 2001), and from time-series cruises along Line-P (e.g., Wong and Chan, 1991). In general, the northeastern subarctic Pacific is thought to be a small sink for atmospheric CO$_2$ (Landrum et al., 1996). Conditions in the northern GOA, however, are likely to be very different. The conditions shoreward of the Alaska Current/Alaska Stream are much more variable than those seaward. None of these carbon programs has sampled the GOA region sufficiently to describe the nutrient/carbon dynamics in this region. The extensive ship-of-opportunity work that has occurred in this area only cuts across the southern boundary of the GOA, between Victoria and Unimak Pass. Perhaps the best indication that conditions in the northern GOA are very different from the generalized assessment of the northeastern subarctic Pacific can be derived from recent high-resolution ship-of-opportunity data (Y. Nojiri, personal communication; http://www.mirc.jha.or.jp/minnano/CGER_NIES/skaugran/index.html). The pCO$_2$ variability observed as the ship transects through Unimak Pass is among the largest observed anywhere in the world (175–185 ppm)—suggesting the importance of localized upwelling events. A proper assessment of this variability can provide valuable information on the physical and biological mechanisms operating in this area.

We close the discussion with consideration of unresolved issues for GOA coastal meteorology and oceanography. First, our results provide some information on along-coast variability. Using the interannual variations from the various locations as a guide (Figs. 5–8), it is apparent that the coherence in the weather along the coast is greater in winter than in summer, especially in terms of the winds. In general, the coherence between the various stations is greatest in the wind time series and least in the precipitation time series. This result is no surprise, in that precipitation has more inherent small-scale variability, and hence more sensitivity to local effects, than does the wind. Even so, there are certainly systematic small-scale variations in GOA coastal winds, especially near gaps in the terrain (as shown by Macklin et al., 1988, 1990). It is uncertain how sensitive the ACC is to these kinds of variations on scales of ~ 100 km, but because the variations are locked to the terrain they tend to be persistent.

Transport from Gore Point through the Shelikof Sea Valley, appears to be coherent, but the continuity of flow from the region east of Kayak Island to the Kenai Peninsula is not known. Satellite-tracked drifters (Fig. 10a) indicate that there likely is an interruption of flow at Kayak Island, and a reorganization along the Kenai Peninsula. In particular, what role this flow plays in supply of nutrients to ACC downstream from the Seward line has only been hypothesized through models. In addition, the ACC is greatly modified by the topography from Kayak Island through Shelikof Strait. The currents on the shallow shelves to the east of the Kodiak Island and the east of the Semidii Islands appear to be more dominated by local processes. Cross-shelf advection is critical to this ecosystem. To understand the mechanisms that control onshelf flux requires focused research on mesoscale processes particularly those involving canyons and eddies.

In general, we have an incomplete understanding of how the coastal weather relates to the large-scale atmospheric circulation. The response of the low-level flow to the coastal terrain depends on factors such as wind speed and static stability, as encapsulated in scaling parameters such as the Froude number, but this response is complicated not just by terrain variations, but also time-dependent effects and non-conservative (diabatic and friction) processes. Progress here requires high-resolution numerical weather prediction model experiments (present models do seem capable of accurately accounting for terrain effects) with sufficient observations for validation. The transport in the ACC is apparently largely controlled by winds; knowledge how spatial variability in wind forcing impacts transport and the confinement of the low salinity water along the shelf is critical in understanding this ecosystem.

In addition, our knowledge of the runoff into the GOA is meager. The hydrology of the region is greatly complicated by factors related to variations in precipitation type (snow or rain) as a function of altitude and location, and freeze/melt cycles on land. Present hydrological models are not up to the task of characterizing the runoff into the GOA, and past and present monitoring of rivers draining into the GOA is poor. If the details of this runoff are important to the ACC, which is likely, a major increase in our hydrological capabilities is required for monitoring, let alone predicting, the freshwater input to the ACC. It must be noted that runoff contributes to micronutrient supply to this marine ecosystem. Quite obviously, measurements of nutrients and sediments provided by rivers should be expanded. Finally, an understanding temporal changes in the climate (interannual, decadal and long-term time scales) and how these changes impact the ecosystem is critical.

From a bottom up perspective, the ultimate control of the complicated ecosystem found in the GOA, lies in how the meteorological forcing controls the ocean physics that in turn governs the availability of nutrients and hence food within the lowest trophic levels. If conditions of runoff, advection, physical mixing, nutrient and light availability change primary production, its timing or the composition of the primary producers, the entire food web structure can be affected (Napp et al., 1996) with perhaps deleterious impacts on the highest trophic levels.

Acknowledgements

We thank D. Kachel for data analysis and S. Salo for providing satellite images. E. Dobbins developed the algorithms used for model float tracking experiments. C. Sabine provided discussion on carbon in the North Pacific. We thank two anonymous reviewers and C. Mooers for their careful reading and comments on this manuscript. K. Birchfield provided graphics work and R. Whitney did the technical editing (all at PMEL). We thank Dr. T. Royer for supplying the run-off time series and UAF for the GAK1 time series. This research was funded by the Coastal Ocean Processes Program at ONR. This is contribution FOCI-0452 to the Fisheries Oceanography Coordinated Investigations; 849 to Joint Institute for the Study of Atmosphere and Ocean, University of Washington, 2343 to PMEL, and 348 to USGLOBEC.

References

Allen, S.E., Vindeirinho, C., Thomson, C.R.E., Foreman, M.G.G., Mackas, D.L., 2001. Physical and biological processes over a submarine canyon during an upwelling event. Canadian Journal of Fisheries and Aquatic Sciences 58, 671–684.

Barnston, A.G., Livezey, R.E., 1986. Classification, seasonality and persistence of low-frequency atmospheric circulation patterns. Monthly Weather Review 115, 1083–1126.

Bitz, C.C., Battisti, D.S., 1999. Interannual to decadal variability in climate and the glacier mass balance in Washington, Western Canada, and Alaska. Journal of Climate 12, 3181–3196.

Bograd, S.J., Stabeno, P.J., Schumacher, J.D., 1994. A census of mesoscale eddies in Shelikof Strait, Alaska, during 1989. Journal of Geophysical Research 99 (C9), 18243–18254.

Bond, N.A., Stabeno, P.J., 1998. Analysis of surface winds in Shelikof Strait, Alaska using moored buoy observations. Weather Forecasting 13, 547–559.

Burrell, D.C., 1987. Interaction between silled fjords and coastal regions. In: Hood, D.W., Zimmerman, S.T. (Eds.), The Gulf of Alaska: Physical Environment and Biological Resources, DOC/NOAA, USA, pp. 187–220.

Chelton, D.B., Davis, R.E., 1982. Monthly mean sea level variability along the western coast of North America. Journal of Physical Oceanography 12, 757–784.

Conkright, T., O' Brien, M., Levitus, S., Boyer, T.P., Antonov, J., Stephens, C., 1998. World Ocean Atlas 1998 Vol. 11: Nutrients and Chlorophyll of the Pacific Ocean. NOAA Atlas NESDIS 37. US Gov. Printing Office, Washington, DC, 245pp.

Dinnel, S.P., Wiseman Jr., W.J., 1986. Freshwater on the Louisiana and Texas shelf. Continental Shelf Research 6, 75–84.

Doyle, J.D., Bond, N.A., 2001. Research aircraft observations and numerical simulations of a warm front approaching Vancouver Island. Monthly Weather Review 129, 978–998.

Enfield, D.B., Allen, J.S., 1980. On the structure and dynamics of monthly mean sea level anomalies along the pacific coast of North and South America. Journal of Physical Oceanography 10, 557–578.

Francis, R.C., Hare, S.R., 1994. Decadal-scale regime shifts in the large marine ecosystems of the Northeast Pacific: a case for historical science. Fisheries Oceanography 3, 279–291.

Freeland, H., Denman, K., Wong, C.S., Whitney, F., Jacques, R., 1997. Evidence of change in the winter mixed layer in the northeast pacific ocean. Deep-Sea Research 44, 2117–2129.

Frost, B.W., 1991. The role of grazing in nutrient-rich areas of the open sea. Limnology and Oceanography 36, 1616–1630.

Gargett, A.E., 1997. The optimum stability window: a mechanism underlying decadal fluctuations in North Pacific salmon stocks? Fisheries Oceanography 6, 109–117.

Gill, A.E., 1982. Atmosphere-Ocean Dynamics. Academic Press, New York, 662pp.

Glass, R.L., 1999. Water-quality assessment of the Cook Inlet Basin, Alaska—Summary of data through 1997. Water-Resources Investigations Report 99-4116, US Geological Survey, Anchorage, AK, 110pp.

Goering, J.J., Patten, C.J., Shiels, W.E., 1973. Nutrient cycles. In: Hood, D.W., Shiels, W.E., Kelley, E.J. (Eds.), Environmental Studies of Port Valdez. Institute of Mar. Studies, Occasional Pub. No. 3, University of Alaska Fairbanks, Fairbanks, AK, pp. 225–248.

Hare, S.R., 1996. Low frequency climate variability and salmon production. Ph.D. Dissertation, University of Washington, School of Fisheries, 306pp.

Hare, S.R., Mantua, N.J., 2000. Empirical evidence for North Pacific regime shifts in 1977 and 1989. Progress in Oceanography 47, 103–145.

Hayes, S.P., 1979. Variability of current and bottom pressure across the continental shelf in the Northeast Gulf of Alaska. Journal of Physical Oceanography 9 (1), 88–103.

Hayes, S.P., Schumacher, J.D., 1976. Description of wind, current and bottom pressure variations on the continental shelf in the Northeast Gulf of Alaska from February–May 1975. Journal of Geophysical Research 81, 6411–6419.

Hermann, A.J., Stabeno, P.J., 1996. An eddy-resolving model of circulation on the western Gulf of Alaska shelf: 1. Model development and sensitivity analyses. Journal of Geophysical Research 101 (C1), 1129–1149.

Hermann, A.J., Hinckley, S., Megrey, B.A., Stabeno, P.J., 1996. Interannual variability of the early life history of walleye Pollock near Shelikof strait as inferred from a spatially explicit, individual-based model. Fisheries Oceanography 5 (Suppl. 1), 39–57.

Hermann, A.J., Haidvogel, D.B., Dobbins, E.L., Stabeno, P.J., 2002. Coupling global and regional circulation models in the coastal Gulf of Alaska. Progress in Oceanography 53 (2–4), 335–367.

Ingraham Jr., W.J., Ebbesmeyer, C.C., Hinrichsen, R.A., 1998. Imminent climate and circulation shift in North Pacific Ocean could have major impact on marine resources. Eos, Transactions of the American Geophysical Union 79, 197–201.

Kalnay, E., Kanamitsu, M., Kistler, R., Collins, W., Deaven, D., Gandin, L., Iredell, M., Saha, S., White, G., Woollen, J., Zhu, Y., Leetmaa, A., Reynolds, B., Chelliah, M., Ebisuzaki, W., Higgins, W., Janowiak, J., Mo, K.C., Ropelewski, C., Wang, J., Jenne, R., Joseph, D., 1996. The NCEP/NCAR 40-year reanalysis project. Bulletin of the American Meteorological Society 77, 437–471.

Klinck, J., 1988. The influence of a narrow transverse canyon on initially geostrophic flow. Journal of Geophysical Research 93, 509–515.

Lackmann, G.M., Overland, J.E., 1989. Atmospheric structure and momentum balance during a gap-wind event in Shelikof Strait, Alaska. Monthly Weather Review 117, 1817–1833.

Lagerloef, G.S.E., 1995. Interdecadal variations in the Alaska Gyre. Journal of Physical Oceanography 25, 2242–2258.

Landrum, L.L., Gammon, R.H., Feely, R.A., Murphy, P.P., Kelly, K.C., Cosca, C.E., Weiss, R.F., 1996. North Pacific Ocean CO2 disequilibrium for spring through summer, 1985–1989. Journal of Geophysical Research 101 (C12), 28539–28555.

Large, W.G., Pond, S., 1982. Sensible and latent heat measurements over the ocean. Journal of Physical Oceanography 12, 464–482.

Larrance, J.D., Chester, A.J., 1979. Source, composition and flux of organic detritus in lower cook inlet. Outer Continental Shelf Environmental Assessment Program, Final Reports of Principal Investigators 46, 1–71.

Larrance, J.D., Tennant, D.A., Chester, A.J., Ruffio, P.A., 1977. Phytoplankton and primary production in the northeast Gulf of Alaska and lower Cook Inlet: Final Report. Research Unit 425. Environmental Assessment of the Alaskan Continental Shelf, Annual Reports of Principal Investigators for the Year Ending March 1977, 10, 1–136.

Macklin, S.A., Lackmann, G.M., Gray, J., 1988. Offshore-directed winds in the vicinity of prince William Sound, Alaska. Monthly Weather Review 116 (6), 1289–1301.

Macklin, S.A., Bond, N.A., Walker, J.P., 1990. Structure of a low-level jet over lower Cook Inlet, Alaska. Monthly Weather Review 118 (12), 2568–2578.

Mantua, N.J., Hare, S.R., Zhang, Y., Wallace, J.M., Francis, R.C., 1997. A pacific interdecadal climate oscillation with impacts on salmon production. Bulletin of the American Meteorological Society 78, 1069–1079.

Martin, J.H., Gordon, R.M., 1988. Northeast pacific iron distributions in relation to primary productivity. Deep-Sea Research 35, 177–196.

Martin, J.H., Gordon, R.M., Fitzwater, S., Broenkow, W.W., 1989. VERTEX: phytoplankton/iron studies in the Gulf of Alaska. Deep-Sea Research 36, 649–680.

Minobe, S., Mantua, N., 1999. Interdecadal modulation of interannual atmospheric and ocean variability over the North Pacific. Progress in Oceanography 43, 163–192.

Munchow, A., 2000. Wind stress curl forcing of the coastal ocean near Point Conception, California. Journal of Physical Oceanography 30, 1265–1280.

Murphy, P.P., Feely, R.A., Wanninkhof, R., 1998. On obtaining high-precision measurements of oceanic $p\mathrm{CO}_2$ using infrared analyzers. Marine Chemistry 62 (1–2), 103–115.

Murphy, P.P., Nojiri, Y., Harrison, D.E., Larkin, N.K., 2001. Scales of spatial variability for surface ocean $p\mathrm{CO}_2$ in the Gulf of Alaska and Bering Sea: toward a sampling strategy. Geophysical Research Letters 28, 1047–1050.

Napp, J.M., Incze, L.S., Ortner, P.B., Siefert, D.L.W., Britt, L., 1996. The plankton of Shelikof Strait, Alaska: standing stock, production, mesoscale variability and their relevance to larval fish survival. Fisheries Oceanography 5 (Suppl. 1), 19–38.

Norris, J.R., Zhang, Y., Wallace, J.M., 1998. Role of low clouds in summertime atmosphere–ocean interactions over the North Pacific. Journal of Climate 11, 2473–2481.

Overland, J.E., Bond, N.A., 1995. Observations and scale analysis of coastal wind jets. Monthly Weather Review 123 (10), 2934–2941.

Overland, J.E., Adams, J.M., Bond, N.A., 1999a. Decadal variability in the Aleutian low and its relation to high-latitude circulation. Journal of Climate 12 (5), 1542–1548.

Overland, J.E., Salo, S., Adams, J.M., 1999b. Salinity signature of the Pacific Decadal Oscillation. Geophysical Research Letters 26 (9), 1337–1340.

Overland, J.E., Bond, N.A., Adams, J.M., 2001. North Pacific atmospheric and SST anomalies in 1997: links to ENSO? Fisheries Oceanography 10, 69–80.

Overland, J.E., Bond, N.A., Adams, J.M., 2002. The relation of surface forcing of the Bering Sea to large-scale climate patterns. Deep-Sea Research II: Topical Studies in Oceanography 49 (26), 5855–5868.

Parish, T.R., 1982. Barrier wind along the Sierra Nevada Mountains. Journal of Applied Meteorology 21, 925–930.

Reeburgh, W.S., Kipphut, G.W., 1987. Chemical distributions and signals in the Gulf of Alaska, its coastal margins and estuaries. In: Hood, D.W., Zimmerman, S.T. (Eds.), The Gulf of Alaska. US Dept. of Commerce, USA, pp. 77–91

Reed, R.K., 1984. Flow of the Alaskan Stream and its variations. Deep-Sea Research 31 (4), 369–386.

Reed, R.K., 1987. Salinity characteristics and flow of the Alaska Coastal Current. Continental Shelf Research 7, 573–576.

Reed, R.K., Schumacher, J.D., 1986. Physical Oceanography. In: Hood, D.W., Zimmerman, S.T. (Eds.), The Gulf of Alaska: Physical Environment and Biological Resources. Ocean Assessment Division, NOAA, USA, pp. 57–75.

Reed, R.K., Stabeno, P.J., 1989. Recent observations of variability in the path and vertical structure of the Alaskan Stream. Journal of Physical Oceanography 19 (10), 1634–1642.

Reed, R.K., Bograd, S.J., 1995. Transport in Shelikof Strait, Alaska: an update. Continental Shelf Research 15 (2/3), 213–218.

Reed, R.K., Schumacher, J.D., Incze, L.S., 1987. Circulation in Shelikof Strait, Alaska. Journal of Physical Oceanography 17 (9), 1546–1554.

Renwick, J.A., Wallace, J.M., 1996. Relationships between North Pacific wintertime blocking, El Niño, and the PNA pattern. Monthly Weather Review 124, 2071–2076.

Royer, T.C., 1979. On the effect of precipitation and runoff on coastal circulation in the Gulf of Alaska. Journal of Physical Oceanography 9, 553–563.

Royer, T.C., 1982. Coastal fresh water discharge in the northeast Pacific. Journal of Geophysical Research 87, 2017–2021.

Royer, T.C., 1981. Baroclinic transport in the Gulf of Alaska. Part II. Fresh water driven coastal current. Journal of Marine Research 39, 251–266.

Royer, T.C., 1998. Coastal Processes in the northern North Pacific. In: Robinson, A.R., Brink, K.H. (Eds.), The Sea, Vol. 11. Wiley, New York, pp. 395–413.

Royer, T.C., Grosch, C.E., 2000. Analysis of low frequency signals in the northeast Pacific coastal freshwater discharge, salinity, temperature an salmon production using wavelet techniques, presented at the Ninth Annual Pices Meeting, Hakodate, Japan 24 October, 2000.

Sambrotto, R.N., Lorenzen, C.J., 1987. Phytoplankton and Primary Production. In: Hood, D.W., Zimmerman, S.T. (Eds.), The Gulf of Alaska. US Department of Commerce, USA, pp. 249–282.

Schumacher, J.D., Reed, R.K., 1980. Coastal flow in the northwest Gulf of Alaska: the Kenai Current. Journal of Geophysical Research 85 (C11), 6680–6688.

Schumacher, J.D., Pearson, C.A., Overland, J.E., 1982. On exchange of water between the Gulf of Alaska and the Bering Sea through Unimak Pass. Journal of Geophysical Research 87 (C7), 5785–5795.

Schumacher, J.D., Stabeno, P.J., Roach, A.T., 1989. Volume transport in the Alaska Coastal Current. Continental Shelf Research 9 (12), 1071–1083.

Schumacher, J.D., Stabeno, P.J., Bograd, S.J., 1993. Characteristics of an eddy over a continental shelf: Shelikof Strait, Alaska. Journal of Geophysical Research 98, 98395–98404.

Sharples, J., Moore, C.M., Rippeth, T.P., Holligan, P.M., Fisher, D.J., Simpson, J.H., 2001. Phytoplankton distribution and survival in the thermocline. Limnology and Oceanography 46, 486–496.

Spencer, R.W., 1993. Global oceanic precipitation from the MSU during 1979–1991 and comparisons to other climatologies. Journal of Climate 6, 1301–1326.

Stabeno, P.J., Reed, R.K., 1991. Recent Lagrangian measurements along the Alaskan Stream. Deep-Sea Research 38 (3), 289–296.

Stabeno, P.J., Hermann, A.J., 1996. An eddy circulation model for the western Gulf of Alaska shelf. II. Comparison of results to oceanographic observations. Journal of Geophysical Research 101, 1151–1161.

Stabeno, P.J., Reed, R.K., Schumacher, J.D., 1995a. The Alaska Coastal Current: continuity of transport and forcing. Journal of Geophysical Research 100, 2477–2485.

Stabeno, P.J., Hermann, A.J., Bond, N.A., Bograd, S.J., 1995b. Modeling the impact of climate variability on the advection of larval walleye pollock (*Theragra chalcogramma*) in the Gulf of Alaska. In: Beamish, R.J. (Ed.), Climate Change and Northern Fish Populations, Can. Spec. Publ. Fish. Aquat. Sci. 121, 719–727.

Stabeno, P.J., Schumacher, J.D., Bailey, K.M., Brodeur, R.D., Cokelet, E.D., 1996. Observed patches of walleye pollock eggs and larvae in Shelikof Strait, Alaska: their characteristics, formations and persistence. Fisheries Oceanography 5 (Suppl. 1), 81–91.

Stabeno, P.J., Reed, R.K., Napp, J.M., 2002. Transport through Unimak Pass, Alaska. Deep-Sea Research II: Topical Studies in Oceanography 49 (26), 5931–5943.

Stephens, M.P., Samuels, G., Olson, D.B., Fine, R.A., Takahashi, T., 1995. Sea-air flux of CO_2 in the North Pacific using shipboard and satellite data. Journal of Geophysical Research 100 (C7), 13571–13583.

Sugai, S.F., Burrell, D.C., 1984. Transport of dissolved organic carbon, nutrients, and trace metals from the Wilson and Blossom Rivers to Smeaton Bay, Southeast Alaska. Canadian Journal of Fisheries and Aquatic Sciences 41, 180–190.

Takahashi, T., Olafsson, J., Goddard, J., Chipman, D.W., Sutherland, S.C., 1993. Seasonal variation of CO_2 and nutrients in the high latitude surface oceans: a comparative study. Global Biogeochemical Cycles 7, 843–878.

Thompson, R.E., Gower, J.F.R., 1998. A basin-scale oceanic instability event in the Gulf of Alaska. Journal of Geophysical Research 103, 3033–3040.

Townsend, D.W, Cammen, L.M., Holligan, P.M., Campbell, D.E., Pettigrew, N.R., 1994. Causes and consequences of variability in the timing of spring phytoplankton blooms. Deep Sea Research 41, 747–765.

USGS Web Page, http://www.waterdata.usgs.gov/ak/nwis/qwdata.

US Navy Marine Climatic Atlas, 1969.

Wallace, J.M., 2000. North Atlantic Oscillation/Annular Mode: Two paradigms? One Phenomenon. Quarterly Journal of the Royal Meteorological Society 126, 791–805.

Wallace, J.M., Gutzler, D.S., 1981. Teleconnections in the geopotential height field during the Northern Hemisphere winter. Monthly Weather Review 109, 784–812.

Wallace, J.M., Smith, C., Bretherton, C.S., 1992. Singular value decomposition of wintertime sea surface temperature and 500-mb height anomalies. Journal of Climate 5, 561–576.

Whitney, F.A., Welch, D.W., 2002. Impact of the 1997–8 El Niño and 1999 La Niña on the nutrient supply in the Gulf of Alaska. Progress in Oceanography 54, 405–421.

Whitney, F.A., Wong, C.S., Boyd, P.W., 1998. Interannual variability in nitrate supply to surface waters of the Northeast Pacific Ocean. Marine Ecology Progress Series 170, 15–23.

Whitney, F.A., Mackas, D.L., Welch, D., Robert, M., 1999. Impact of the 1990's El Niños on nutrient supply and productivity of Gulf of Alaska waters. In: Proceedings of the 1998 Science Board Symposium on the Impacts of the 1997/98 El Niño Event on the North Pacific Ocean and its Marginal Seas, Pices Scientific Report No. 10, pp. 59–62.

Wilson, J.G., Overland, J.E., 1986. Meteorology of the northern Gulf of Alaska. In: Hood, D.W., Zimmerman, S.T.

(Eds.), The Gulf of Alaska: Physical Environment and Biological Resources, DOC/NOAA, DOI, pp. 31–54.

Wong, C.S., Chan, Y.H., 1991. Temporal variations in the partial pressure and flux of CO_2 at ocean station P in the subarctic Northeast Pacific Ocean. Tellus 43B, 206–223.

Woods, J., Barkmann, W., 1993. The plankton multiplier—positive feedback in the greenhouse. Journal of Plankton Research 15, 1053–1074.

Zhang, Y., Wallace, J.M., Battisti, D.S., 1997. ENSO-like interdecadal variability. Journal of Climate 10, 1004–1020.